Calibration of hydroclimate proxies in freshwater bivalve shells from Central and West Africa

Zita Kelemen [a,b,*], David P. Gillikin [b], Lauren E. Graniero [b,c], Holly Havel [b], François Darchambeau [d], Alberto V. Borges [d], Athanase Yambélé [e], Alhou Bassirou [f], Steven Bouillon [a]

[a] *Department of Earth & Environmental Sciences, KU Leuven, Celestijnenlaan 200E, 3000 Leuven, Belgium*
[b] *Department of Geology, Union College, 807 Union St., Schenectady, NY 12308, USA*
[c] *Department of Geological Sciences, University of North Carolina Chapel Hill, 104 South Road, Chapel Hill, NC 27571-0035, USA*
[d] *Chemical Oceanography Unit, University of Liège, Allée du 6 Août, 17 (Bât B5), 4000 Liège, Belgium*
[e] *Service de l'Agrométéorologie et de Climatologie, Direction de la Météorologie Nationale, Bangui, Central African Republic*
[f] *Département des Sciences de la Vie et de la Terre, Université Abdou Moumouni, Niamey, Niger*

Abstract

Freshwater bivalve shell oxygen and carbon stable isotope ratios ($\delta^{18}O$, $\delta^{13}C$) may act as recorders of hydroclimate (e.g., precipitation-evaporation balance, discharge) and aquatic biogeochemistry. We investigate the potential of these hydroclimate proxies measured along the growth axis of shells collected from the Oubangui River (Bangui, Central African Republic) and the Niger River (Niamey, Niger). Biweekly water samples and *in situ* measurements collected over several years, along with daily discharge data from both sites allowed a direct comparison with proxies recorded in the shells. Data from a total of 14 unionid shells, including three species (*Chambardia wissmanni*, *Aspatharia dahomeyensis*, and *Aspatharia chaiziana*), confirmed that shells precipitate carbonate in oxygen isotope equilibrium with ambient water. Because water temperature variations were small, shell $\delta^{18}O$ values ($\delta^{18}O_{shell}$) also accurately record the seasonality and the range observed in water $\delta^{18}O$ ($\delta^{18}O_w$) values when calculated using an average temperature. Calculated $\delta^{18}O_w$ values were in good agreement over the entire record of measured $\delta^{18}O_w$ values, thus $\delta^{18}O_{shell}$ records can be reliably used to reconstruct past $\delta^{18}O_w$ values. Discharge and $\delta^{18}O_w$ values from both rivers fit a logarithmic relationship, which was used to attempt reconstruction of past hydrological conditions, after calculating $\delta^{18}O_w$ values from $\delta^{18}O_{shell}$ values. A comparison with measured discharge data suggests that for the two rivers considered, $\delta^{18}O_{shell}$ data are good proxies for recording discharge conditions during low(er) discharge levels, but that high discharge values cannot be accurately reconstructed due to the large scatter in the discharge-$\delta^{18}O_w$ relationship. Moreover, periods of bivalve shell growth cessation due to high turbidity or air exposure should be taken into account. While $\delta^{13}C$ values of dissolved inorganic carbon in both rivers showed clear seasonality and correlated well with discharge, most of the shells analyzed did not record these variations adequately, likely due to the complication of vital effects including the variable contribution of metabolic CO_2. Thus, tropical African unionid $\delta^{18}O_{shell}$ values can be used to reconstruct $\delta^{18}O_w$ values with high confidence to provide insight on past hydroclimate such as precipitation-evaporation balance and periods of low discharge.

* Corresponding author at: Department of Earth & Environmental Sciences, KU Leuven, Celestijnenlaan 200E, 3000 Leuven, Belgium.
  E-mail address: zita.kelemen@kuleuven.be (Z. Kelemen).

1. INTRODUCTION

Changes in the hydrological cycle are sensitive markers of ongoing climate change and anthropogenic impact on the environment. Predicted global fluctuations in climate are expected to have strong environmental impacts on continental Africa (De Wit and Stankiewicz, 2006) that will be amplified by anthropogenic driven land-use change (Descroix et al., 2012; Lawrence and Vandecar, 2015). Many of the factors involved in climate change also directly affect the hydrological cycle, which in turn change the characteristics of river systems; particularly annual discharge amounts and/or the seasonality in discharge (Itiveh and Bigg, 2008; Mahé et al., 2013; Aich et al., 2014). In addition, river systems are experiencing increased pressure from urbanization, water abstraction, and the construction of reservoirs (Snoussi et al., 2007). Thus, river discharge data can provide sensitive information about local or regional changes in climate or land-use. Direct measurements of the water geochemistry, hydrology, and material fluxes in African river systems have historically been scarce (Laraque et al., 2001; Runge and Nguimalet, 2005; Coynel et al., 2005; Bouillon et al., 2012), but they are extremely valuable for monitoring the functioning of river basins. These long-term datasets are paramount to detect trends in riverine material fluxes and/or hydrology. In the absence of long-term monitoring programs and datasets, reliable proxies are needed to reconstruct past conditions in order to detect persisting trends.

The potential of bivalve shells as archives of precipitation patterns (e.g., monsoon duration, droughts, etc.), (paleo)temperature, and pollution has been recognized in a diverse range of studies (Abell et al., 1996; Dettman et al., 1999, 2001, 2004; Dettman and Lohmann, 2000; Goodwin et al., 2003; Gillikin et al., 2005a,b, 2006, 2008; Fan and Dettman, 2009; Gordillo et al., 2011; Azzoug et al., 2012; Vonhof et al., 2013; O'Neil and Gillikin, 2014). Bivalves store information on the geochemical and environmental conditions of their habitat in sequentially deposited shell carbonate and serve as good candidates to circumvent the absence of historical data (Gröcke and Gillikin, 2008). Sequentially secreted layers do not only contain information about salinity, temperature, and hydrology, but can also be used to infer the age and growth rates of the bivalve itself (Goodwin et al., 2001; Wanamaker et al., 2007). Freshwater bivalve shells have the potential to provide a useful substrate to reconstruct past rainfall or river discharge patterns, as shell aragonite has been shown to precipitate in oxygen isotopic equilibrium with the ambient water (Grossman and Ku, 1986; Dettman et al., 1999) and the oxygen isotope composition of river water ($\delta^{18}O_w$) is related to precipitation and evaporation (Dansgaard, 1964; Mook and Rozanski, 2000), which often shows a clear relationship with discharge (Ricken et al., 2003; Dettman et al., 2004; Versteegh et al., 2011). While the degree of isotope fractionation between water and aragonite is temperature-dependent, changes in $\delta^{18}O_w$ values should be the dominant driver of variations in shell $\delta^{18}O$ values in tropical regions where water temperature variations are typically small, such as in tropical Africa.

It has been previously established that $\delta^{18}O$ values of freshwater bivalve aragonite can, in certain rivers, be used to efficiently reconstruct river discharge (Ricken et al., 2003; Dettman et al., 2004; Versteegh et al., 2011), but no attempt has been made to validate or apply this approach to tropical African rivers. In order to verify the utility of freshwater bivalve shells as archives of past environmental reconstructions, more robust calibration datasets are needed that combine (i) discharge and geochemistry data of rivers at high temporal resolution, and (ii) high-resolution measurements of stable isotope and/or elemental ratios in shells, whereby the growth period of the shells coincides or overlaps with the period of riverine data collection. Therefore, in this study, we used a large dataset collected over three consecutive years at fortnightly intervals in two large African river systems, the Niger and Oubangui, and compared these with the $\delta^{18}O$ and $\delta^{13}C$ values from serially sampled freshwater bivalve shells collected at the same sites during and after the river monitoring period. These two river systems have contrasting catchment areas, vegetation, and total discharge, but both have well defined seasonality in discharge, and available long-term daily discharge datasets (Orange et al., 1997; Wesselink and Orange, 1996; Laraque et al., 2001; Runge and Nguimalet, 2005; Descroix et al., 2012; Bouillon et al., 2012, 2014). Our objectives were to (i) verify whether African freshwater bivalves secrete carbonate in oxygen and carbon isotope equilibrium with the water in which they live, (ii) determine if $\delta^{18}O_{shell}$ values record $\delta^{18}O_w$ values considering the small variation in water temperature, and (iii) whether tropical freshwater bivalve shells indirectly record the river discharge based on relationships between discharge and $\delta^{18}O_w$ values. This calibration dataset is critical in establishing the robustness of stable isotope proxies in freshwater bivalve shells in contrasting tropical rivers and across different bivalve species, as well as pointing out possible caveats in data interpretation.

2. MATERIALS AND METHODS

2.1. Sampling sites and water sampling

The Oubangui River is the third largest tributary of the Congo River, with a catchment area of 490,000 km^2 upstream of Bangui, and is one of the few sites within the Congo Basin for which a long-term discharge record is available (Orange et al., 1997; Wesselink and Orange, 1996; Laraque et al., 2001; Runge and Nguimalet, 2005). The Oubangui ecoregion is covered by a variety of vegetation types, with humid rain forests in the south and savannas and semi-humid forest dominating in the north (Mayaux et al., 1999). The basin (Fig. 1) has a transitional tropical regime with annual rainfall of 1400–1800 mm yr^{-1}, and a single peak discharge period (Coynel et al., 2005). The lowest discharge is measured after the dry season, during March and April, while the high water period is between September and December. Rainfall in the basin
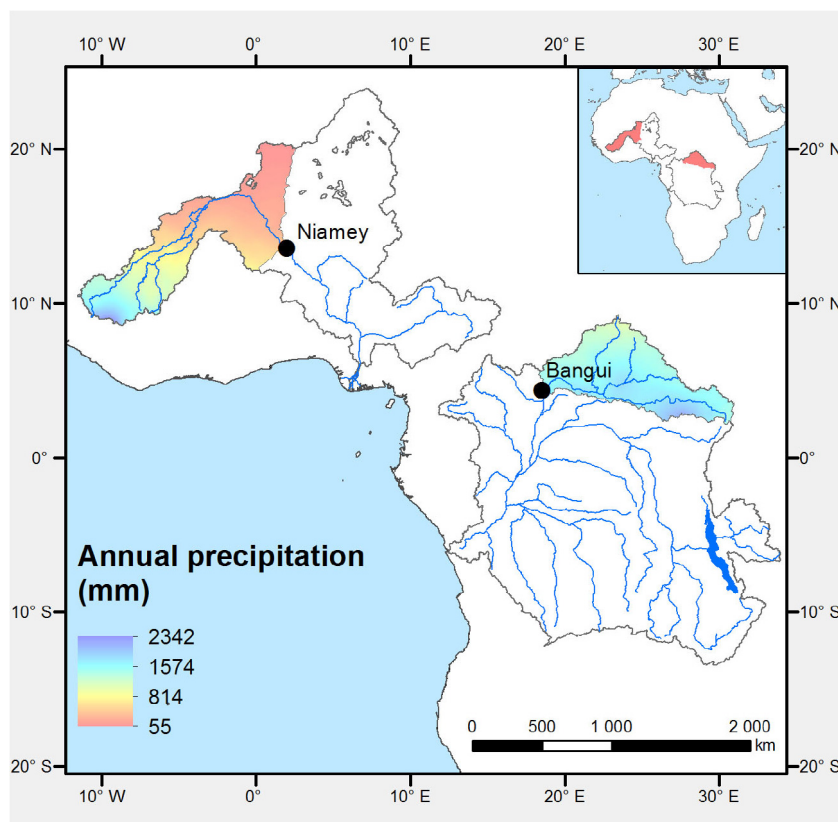
Fig. 1. Map showing the location of the Oubangui and Niger River basins, and the monitoring/sampling sites (black circles). The color scale shows mean annual precipitation in the watershed above the sampling site (data from Hijmans et al., 2005). (For interpretation of the references to colour in this figure legend, the reader is referred to the web version of this article.)

is influenced by the North African air mass, which has historically caused several periods of decreased rainfall after the "wet period" from 1960 to 1970 (Nicholson, 2000). Laraque et al. (2001) determined that during this wet period, a 1% increase in rainfall resulted in an average 18% increase in discharge. In contrast, during the following decade (1971–1981), the precipitation decreased by 3% relative to the mean annual rainfall of the previous 10 years, resulting in a strong (27%) decrease in discharge. In the following decade (1982–1993), the drought continued, resulting in an additional 2% decrease in rainfall and 25% decrease in discharge. The centennial minimum annual discharge was recorded in 1990, measuring only 2120 $m^3 s^{-1}$ (Orange et al., 1997). Despite the small recovery of rainfall in the early 1990s, the drought is ongoing. The drought's evolution is marked by a persistent deficit of flows; since the continuous measurements started in 1935, a 29% decrease in discharge has been recorded (Nguimalet and Orange, 2013). The watershed geology is likely to contribute to the high sensitivity of discharge to the rainfall deficit, given the basin's geological structure is mainly a vast peneplanation surface with soil hardened by a ferruginous cuirass, which favours water runoff (Negrel and Dupre, 1993). Furthermore, the north bank of the Oubangui River lacks sandy soil areas which would otherwise function as aquifers. Land-use change is not expected to have exerted

a strong impact on the watershed hydrology, given the low rates of deforestation and the low population density; although the population increased 150% between 1988 and 2006, the increase in cultivated area still only represents 3% of the total basin area (Nguimalet and Orange, 2013). Nevertheless, the wooded savannas in the north are 'derived savannas' resulting from anthropogenic disturbances, such as fire, and clearance for grazing, timber, and agriculture (Sankaran et al., 2005; Bucini and Hanan, 2007).

The Niger River is the third longest river on the African continent, with a length of 4200 km. The active catchment area is about 1.5 million km^2 and is often divided into four hydrological subcatchment areas: the Upper Niger Basin, the Inland Delta, the Middle Niger Basin, and the Lower Niger Basin, each distinguished by unique topographic and drainage characteristics (Olomoda, 2012). The river supports hydropower generation, irrigated agriculture, fishing, navigation, and is a crucial factor for the economy in West Africa. Our work focuses on the Middle Niger (Fig. 1), with a total catchment area of 700,000 km^2, from which about 400,000 km^2 is active (Amogu et al., 2010). The Middle Niger is located in the Sahelian zone, where the rainfall ranges from 200 mm in the north to 700 mm in the south, mostly dependent on the movement of the intertropical convergence zone (ITCZ). The rainy season starts in May and ends in October, with 90% of annual

rainfall concentrated between June and September (Leduc et al., 2001). The river gauge station at Niamey (Niger) has been in use since 1929, and recorded a maximum discharge in 1968 (2360 $m^3 s^{-1}$) and a minimum discharge in June 1985 when the river experienced no flow at Niamey. The Middle Niger has a two–peak hydrograph, the first peak appearing in September ("red flood") soon after the local rainy season, and the second beginning in December ("black flood") with the arrival of the delayed flood from upstream, when the discharge peak from Guinean rain is slowly released from the Inner Delta in Mali (Descroix et al., 2013). The bi-modal hydrograph of Niger River at Niamey is recent, occurring only in the past few decades. The drought of the 1970s and 1980s, caused by a persistent rainfall deficit, coincided with an increase in runoff and discharge. This paradoxical situation has been attributed to a decrease in the water holding capacity of soils and basins, which could be caused by land use changes, especially land clearing, fallow shortening, and soil crusting (Mahé and Paturel, 2009; Descroix et al., 2009, 2012).

Oubangui River water samples were taken fortnightly between March 2010 and November 2012 in Bangui (Central African Republic). Samples were collected by a custom-made flow-through sampling bottle submerged 0.5 m below the water surface from which 12 ml Labco Exetainer vials were filled, poisoned with $HgCl_2$ and capped without headspace. All samples were shipped to KU Leuven and analyzed for water stable isotopes ($\delta^{18}O_w$) and $\delta^{13}C$ values of dissolved inorganic carbon ($\delta^{13}C_{DIC}$). $\delta^{18}O_w$ was measured by equilibration with CO_2 using an Elemental Analyzer Flash HT coupled to a ThermoFinningan Delta V Advantage isotope ratio mass spectrometer (EA-IRMS) (described in Gillikin and Bouillon, 2007) or a ThermoFinnigan GasBench coupled with ThermoFinnigan Delta V Advantage IRMS (GB-IRMS). For analysis, a 0.5 ml water sample was transferred into 12 ml Labco Exetainer, flushed with helium, and 200 μL (for EA-IRMS) or 35 μL (for GB-IRMS) of pure CO_2 was manually added. Samples were equilibrated at ambient laboratory temperature (EA-IRMS) or at 25 °C in the thermostated tray (GB-IRMS) for over 24 h. Concurrent with river samples, 3 in-house water standards ($\delta^{18}O = +6.87‰$; $-7.19‰$ and $-22.31‰$; normalized to VSMOW/SLAP scale) were measured to correct $\delta^{18}O$ values. All water samples were reanalyzed by the IAEA (International Atomic Energy Agency, Vienna), where water samples were pipetted into 2 ml vials, and measured twice on different laser water isotope analyzers (Los Gatos Research or Picarro). Isotopic values were determined by averaging isotopic values from the last four out of nine injections, along with memory and drift corrections, with final normalization to the VSMOW/SLAP scales by using 2-point lab standard calibrations, as fully described in Wassenaar et al. (2014) and Coplen and Wassenaar (2015). The long-term uncertainty for standard $\delta^{18}O$ values was ±0.1‰. In addition, we expanded our $\delta^{18}O_w$ database using data provided by the IAEA (taken from the Global Network of Isotopes in Rivers (GNIR) database, freely available at http://www-naweb.iaea.org/napc/ih/IHS_resources_gnir.html, for the period between

September 2009 and December 2013). For $\delta^{13}C_{DIC}$ analysis, a 2 ml helium headspace was created, and the remaining water sample was acidified with 99% H_3PO_4 (Sigma Aldrich) to fully convert DIC into CO_2. Samples were left to equilibrate overnight, and the headspace was injected into the EA-IRMS. $\delta^{13}C_{DIC}$ data were corrected for isotopic fractionation between dissolved and gaseous CO_2 and calibrated using certified reference materials LSVEC and NBS 19 (see Gillikin and Bouillon, 2007 for more details). More extensive data on the geochemistry of the Oubangui derived from this sampling effort have been presented elsewhere (Bouillon et al., 2012, 2014). Daily discharge data have been measured since the early 20th century at Bangui, and data were provided by the Direction de la Métérologie Nationale. The monitoring site in the Niger River at Niamey (Niger) was established in April 2011, and water samples for isotope analyses were collected fortnightly until March 2013, and were analyzed as described above. The discharge at Niamey has been recorded since 1929, and data were provided by The Global Runoff Data Centre (Koblenz, Germany). Water temperature in both rivers was recorded using YSI ProPlus probes during each of the sampling events, and was also recorded every two hours over the monitoring period using duplicate HOBO Water Temperature Pro v2 data loggers (U22-01; Onset Computer Corp.).

2.2. Shell collection and analyses

In the Oubangui River, shells were collected on four different occasions during the monitoring period at Bangui: March 2011, February 2012, November 2012, and March 2013. All nine shells used in this study from the Oubangui belong to the species *Chambardia wissmanni* (Table 1). In the Niger River, shells were collected in April 2013, and included one *Aspatharia chaiziana*, two *C. wissmanni* and two *Aspatharia dahomeyensis* specimens (Table 1). All were collected alive, so that data from the last period of growth (i.e., the collection date) can be aligned with the available water data. All species are currently listed as 'Least Concern' by the IUCN (http://www.iucnredlist.org) and seemed abundant at the collection localities. Images of the three species analyzed are available as supplementary material (Figs. S1–S3).

One valve of each shell was sectioned along the maximal growth axis to maximize temporal resolution. Shell sections of a few mm thickness were mounted on glass slides, and the prismatic layer was serially sampled in cross-section from the commissure to the umbo using a New Wave Micromill. Sampling continued until the prismatic layer was either too thin to sample, or was eroded. We used a 300 μm diameter drill bit, with a spot sampling resolution between 350 and 1000 μm and 300 μm depth (see Table 1). This resolution resulted in 30–260 samples per shell – depending on the size of the bivalve – with a sample mass between 50 and 80 μg. Each aragonite powder microsample was collected separately in a 12 ml round-bottom Labco Exetainer. Samples were analyzed either at Union College or KU Leuven on a Thermo Delta V Advantage isotope ratio mass spectrometer coupled to a GasBench

Table 1
Data from all analyzed bivalves, including sample code, species, collection date and total number of samples drilled per specimen (n), with the corresponding sampling resolution in micrometers, shell length and height in millimeters and the estimated age based on the number of cycles in the oxygen stable isotope record.

	Shell code	Species	Collection date (dd/mm/yyyy)	n	Sampling resolution (μm)	Length (mm)	Height (mm)	Estimated age
Niger River (Niamey)	N10A	*A. chaiziana*	27/04/2013	98	350	62	41	~2
	N37B	*A. dahomeyensis*	27/04/2013	90	350	52	26	>2
	N50A	*A. dahomeyensis*	27/04/2013	84	350	47	24	~2
	N14B	*C. wissmanni*	27/04/2013	170	350	90	58	>10
	N8A	*C. wissmanni*	27/04/2013	99	450	97	63	>8
Oubangui River (Bangui)	B17	*C. wissmanni*	18/03/2011	160	350	120	81	>8
	B11	*C. wissmanni*	18/03/2011	29	800	65	40	~2
	B23	*C. wissmanni*	18/03/2011	33	1000	95	60	>2
	B16	*C. wissmanni*	18/03/2011	69	350	85	48	>4
	BB6	*C. wissmanni*	25/11/2012	57	750	95	60	>2
	3B	*C. wissmanni*	11/02/2012	233	350	110	76	>9
	1A	*C. wissmanni*	23/03/2013	103	350	84	45	>5
	2B	*C. wissmanni*	23/03/2013	156	350	85	44	>6
	4A	*C. wissmanni*	23/03/2013	58	350	85	44	>5

II. In both laboratories, Exetainers were flushed with helium and reacted with >100% phosphoric acid to produce CO_2 gas. Samples were allowed to react for >3 h at either 70° or 50 °C, or for 24 h at 25 °C to reach isotope equilibrium. Data from each run were corrected using the regression method with LSVEC ($\delta^{18}O = -26.7‰$, $\delta^{13}C = -46.6‰$), NBS-18 ($\delta^{18}O = -5.01‰$, $\delta^{13}C = -23.2‰$), and NBS-19 ($\delta^{18}O = -2.2‰$, $\delta^{13}C = +1.95‰$) as standards, or using two in-house $CaCO_3$ standards which were regularly calibrated against NBS-19 and LSVEC and whose long-term standard deviations were better than 0.1‰. Both $\delta^{18}O$ and $\delta^{13}C$ values of shell aragonite are expressed relative to the VPDB (Vienna Pee Dee Belemnite) scale, and have precisions of <0.1‰. Mantle and muscle tissues were dissected from recently collected animals, air-dried and homogenized with a mortar and pestle. About 0.8–1.2 mg was weighed into a tin cup, folded, and analyzed for $\delta^{13}C$ on the EA-IRMS. Simultaneously with the tissue samples, IAEA-CH6 and an internally calibrated acetanilide were analyzed and used to calibrate the $\delta^{13}C$ data. Reproducibility of the $\delta^{13}C$ measurements was better than ±0.2‰.

2.3. Predicted shell $\delta^{18}O$ values

Measured values of water temperature and $\delta^{18}O_w$ were used to calculate the expected shell $\delta^{18}O$ ($\delta^{18}O_{shell}$) values (here forth termed the model shell), using the equation for biogenic aragonite isotope fractionation calculated by Dettman et al. (1999) using data from Grossman and Ku (1986):

$$1000 \ln(\alpha) = 2.559(10^6 T^{-2}) + 0.715 \qquad (1)$$

where T is the water temperature in degrees Kelvin and α is the fractionation between water and aragonite described by the following equation:

$$\alpha_{(aragonite-water)} = \frac{1000 + \delta^{18}O_{aragonite}(\text{VSMOW})}{1000 + \delta^{18}O_{water}(\text{VSMOW})} \qquad (2)$$

Water $\delta^{18}O$ values are calculated relative to VSMOW, therefore an additional conversion is necessary to compare shell aragonite values (which are expressed relative to VPDB) to predicted shell values. To convert $\delta^{18}O$ values from the VSMOW to the VPDB scale, $\alpha_{(\text{VSMOW-VPDB})} = 1.0309$ (Gonfiantini et al., 1995) was used.

Measured $\delta^{18}O_{shell}$ values were tuned to calculated model shell $\delta^{18}O$ values using Julian days as the unit for the temporal scale, and using January 1st, 2010 as $t = 0$ (see for example, Klein et al., 1996; Dettman et al., 1999; Gillikin et al., 2005a,b; Goewert et al., 2007; Goodwin et al., 2010; and many others). Using the model shell as a base, $\delta^{18}O_{shell}$ values were manually aligned one by one starting from the first sample drilled at the commissure (ventral shell tip) from each specimen, which was matched with the closest corresponding model shell $\delta^{18}O$ value to the collection date. Subsequent samples were tuned to the model shell according to the chronology of sampling from the commissure towards the umbo (from the most recently precipitated carbonate towards the older layers).

3. RESULTS

3.1. Discharge regimes of the Oubangui and Niger Rivers

The Oubangui River has a transitional tropical regime, featuring a single discharge peak during the wet season, between September and November and lowest flow conditions between March and April. During the monitoring period the highest discharge measured was $8868 \, m^3 \, s^{-1}$ (November 19th, 2012), and a minimum of $265 \, m^3 \, s^{-1}$ was recorded on April 6th, 2012 (Fig. 2A).

During the monitoring period, the highest discharge at Niamey (Niger River) was measured on 2 September 2012 ($1963 \, m^3 \, s^{-1}$), as the highest peak during the first flooding event, and the lowest on 3 June 2012, at the end of dry period ($75 \, m^3 \, s^{-1}$) (Fig. 2B). While Niamey is located in the Sahelian region, with less than $700 \, mm \, year^{-1}$ of rain, the discharge in the Middle Niger is mainly provided by rivers in the Sudanian climatic region, with $700–1400 \, mm \, year^{-1}$

rainfall. The discharge in the Middle Niger River is mainly rain fed, partly from local runoff and partly from flow from Upper Niger and Inner Delta. The first peak discharge period appears during the local rainy season in August to October, while the second (delayed) discharge peak arrives in early December and lasts until February.

3.2. Temperature, $\delta^{18}O_w$ and $\delta^{13}C_{DIC}$ values

For the Oubangui River, we used $\delta^{18}O_w$ and $\delta^{13}C_{DIC}$ values and temperature data collected biweekly between March 2010 and November 2012. Additional $\delta^{18}O_w$ data were provided by the IAEA GNIR database (2009–2013). Jointly, this provided 5 years of consecutive data at monthly or biweekly resolution. The records from 5 years of monitoring show an average $\delta^{18}O_w$ value of $-0.7‰$, and range between $-3.7‰$ and $+2.6‰$ ($n = 112$). The annual variations were pronounced, with higher values during the dry season and lower values at the time of the wet
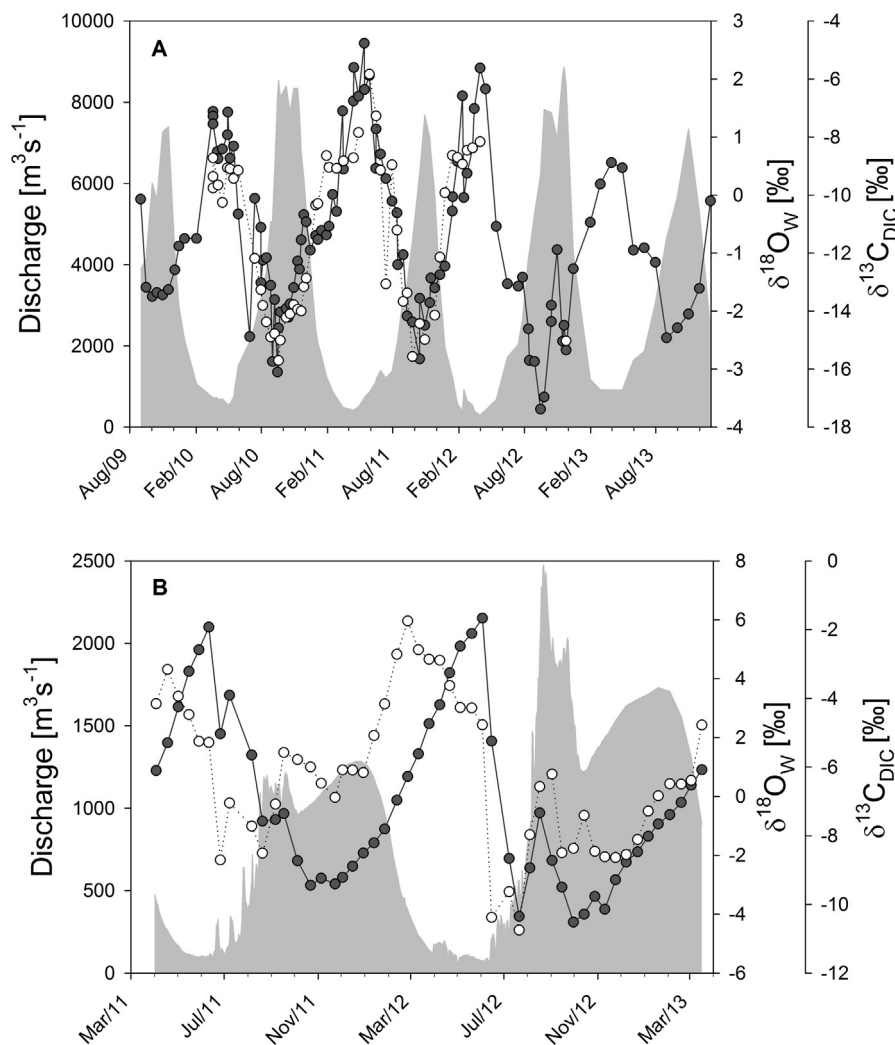

Fig. 2. Daily discharge (grey-shaded area) plotted with measured $\delta^{18}O_w$ (black circles) and $\delta^{13}C_{DIC}$ (open circles) values for (A) the Oubangui River at Bangui, and (B) the Niger River at Niamey during the monitoring periods.

seasons (Fig. 2A). The $\delta^{13}C_{DIC}$ values ranged between −15.7 and −5.8‰ and followed the seasonality of $\delta^{18}O_w$ data with a clear relationship to discharge. The highest $\delta^{13}C_{DIC}$ values were recorded during low discharge, and the lowest values during high discharge conditions. Water temperatures varied between 25.1 and 31.5 °C (average 28.6 ± 1.2 °C), showing an annual trend of lowest values after the wet season from November to January, and highest values in March and April, when the discharge level was the lowest (Fig. 3A). Measurements during the biweekly monitoring agreed well with data from the continuously

recorded temperature (Fig. 3A). The lowest temperatures were measured during short cool periods in January in both 2011 and 2012. Without these short-term exceptions, the water temperature did not fall below 27 °C.

For the Niger River at Niamey, $\delta^{18}O_w$ values ranged between −4.3 and +6.1‰, with an average of −0.1‰ ($n = 50$). The highest value for $\delta^{18}O_w$ was measured at the end of dry season in 2012 (3 June) while the lowest value coincided with the end of first flooding on 30 Sept 2012. $\delta^{13}C_{DIC}$ values ranged between −10.8 and −1.8‰ with highest values measured shortly after the second discharge
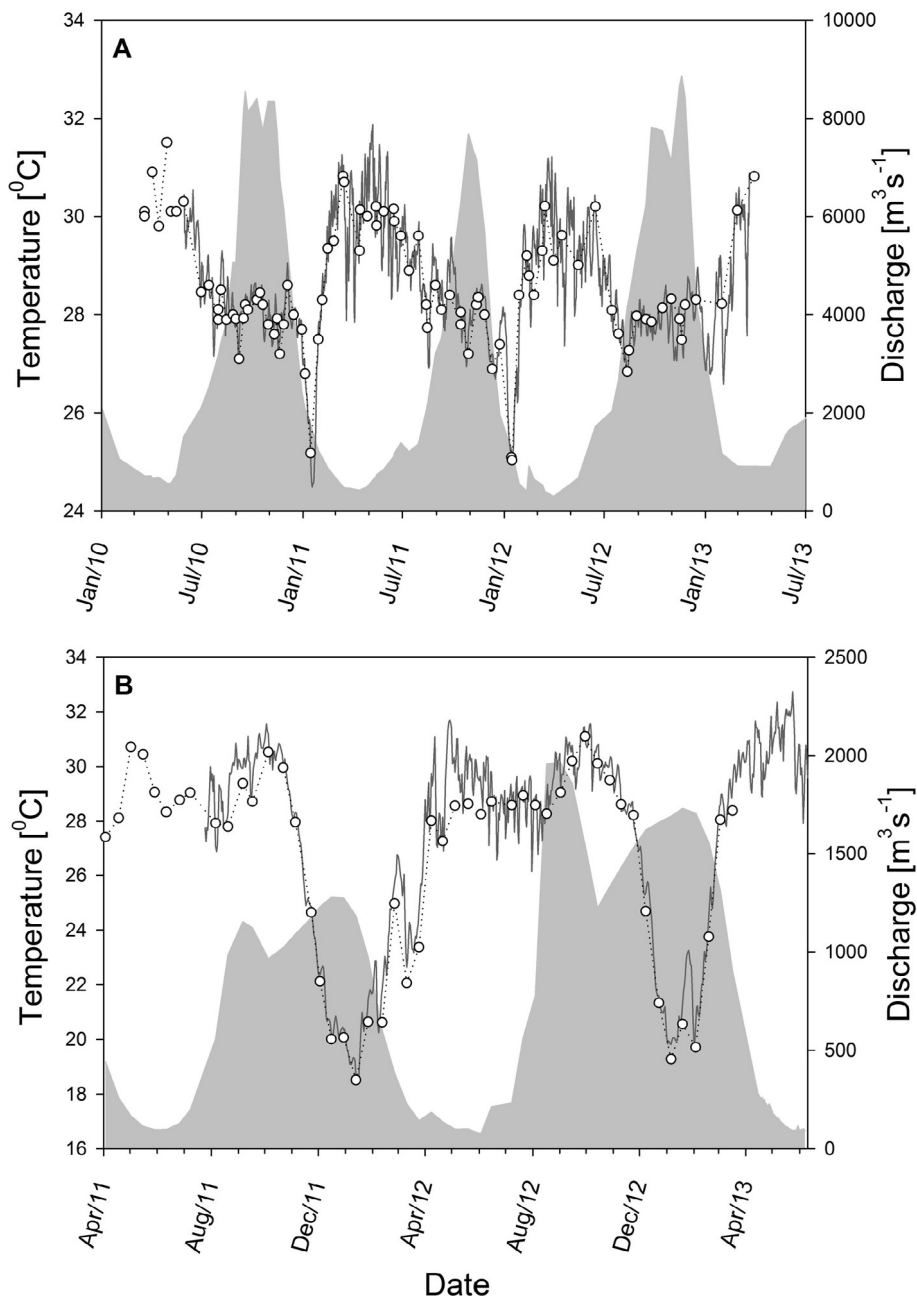

Fig. 3. Daily discharge (grey-shaded area) plotted with water temperature variations in (A) the Oubangui River at Bangui, and (B) the Niger River at Niamey. The solid line represents data from continuous measurements (data loggers, see text), open circles and dashed line represent discrete measurements during biweekly sampling.

Table 2
Carbon isotope data ($\delta^{13}C_{shell}$) from all analyzed bivalves.

	Shell code	Average (‰)	Min (‰)	Max (‰)
Niger River	N10A	−8.2	−10.9	−3.8
	N37B	−8.7	−13.5	−6.1
	N50A	−7.9	−11.0	−5.1
	N14B	−7.9	−10.6	−5.7
	N8A	−8.0	−10.1	−5.7
Oubangui River	B17	−11.1	−13.7	−8.6
	B11	−10.9	−13.3	−9.1
	B23	−10.7	−14.6	−8.2
	B16	−9.8	−11.3	−8.4
	BB6	−11.4	−14.2	−8.7
	3B	−11.5	−14.6	−8.8
	1A	−10.3	−12.9	−8.9
	2B	−10.2	−13.1	−8.6
	4A	−10.6	−12.7	−8.7

peak, in the beginning of the dry season (Fig. 2B). The relationship between discharge and $\delta^{13}C_{DIC}$ values was not as clear as in the Oubangui River, albeit as a general pattern, during low discharge the $\delta^{13}C_{DIC}$ values were elevated while during high discharge they stayed low(er). Water temperature ranged from 18.5 to 31.1 °C (average 26.6 ± 3.7 °C), with lowest temperatures between December and early March (during the black flood) when the air temperature in the area can drop to 10–15 °C (Cappelaere et al.,

2009), while the highest temperatures were recorded during September and October (Fig. 3B). The wider range of measured water temperature reflects the complexity of the Niger River hydrograph. Fig 3B illustrates that water temperature stayed elevated and constant during the first flood peak, when the discharge is fed mainly by local rainfall. During the second flooding, when the discharge is derived from the upper Niger, the water temperature decreased to its minimum of about 19 °C.
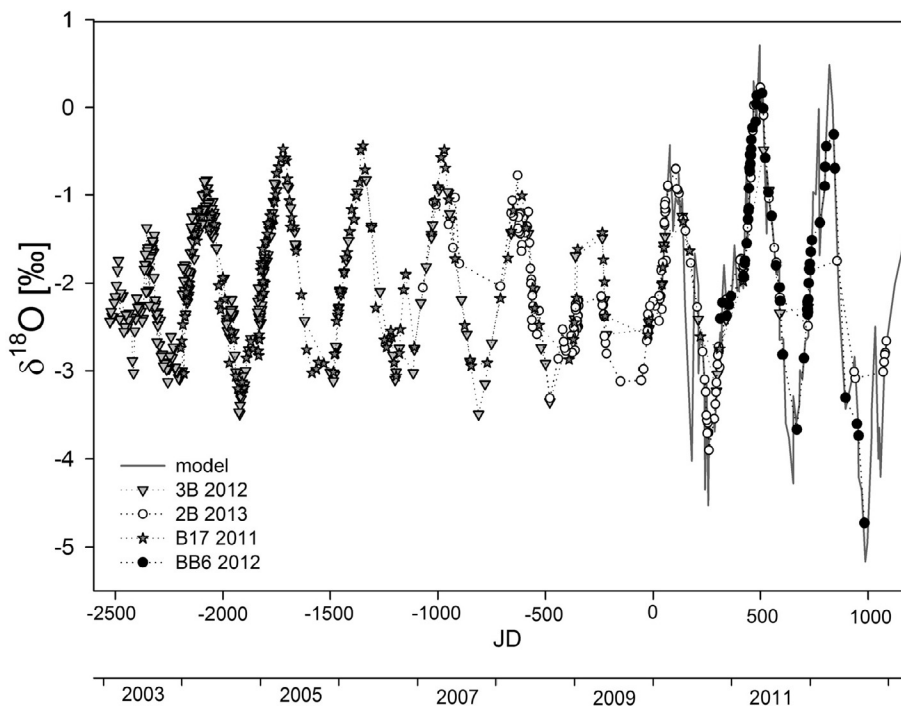

Fig. 4. Oxygen isotope records from four *C. wissmanni* shells collected from the Oubangui River (various symbols representing different specimens), representing each collection event (2011, 2012 March, 2012 September and 2013), and plotted with model shell (solid grey line). The primary *x*-axis represents the Julian date (JD) used for matching actual shell values with the model shell calculated from water data. Note that negative Julian dates are rough approximations because there was no model shell to match these samples with. The secondary *x*-axis is the calendar year spanning the lifetime of the oldest shell. The remainder of the Oubangui River shell data can be found in the supplement.

3.3. Stable isotope profiles of freshwater shells

$\delta^{18}O_{shell}$ values showed a clear cyclicity in both sites and were in good agreement between shells within sites, following the seasonality observed in $\delta^{18}O_w$ values. Shells from the Oubangui River had a $\delta^{18}O$ value range between −5.1 and +0.2‰, whereas values from Niger River shells exhibited a larger amplitude, ranging from −7.8 to +5.8‰. The co-variation between the $\delta^{18}O$ and $\delta^{13}C$ of shells was very poor (Figs. S4 and S5; supplementary material): while $\delta^{18}O_{shell}$ mirrored the seasonal pattern of $\delta^{18}O_w$ values, $\delta^{13}C_{shell}$ values tended to show a decrease through ontogeny in some specimens, independent of seasonal cyclicity. $\delta^{13}C_{shell}$ values also differed between the two sites, ranging between −14.6 and −8.2‰ for the Oubangui River shells (Table 2 and Fig. S4, supplementary material) and −13.5 and −3.8‰ for the Niger River shells (Table 2 and Fig. S5, supplementary material). Gill, mantle and muscle tissues from 44 specimens from Oubangui River and nine specimens from the Niger River were sampled for stable isotope analysis. Soft tissue $\delta^{13}C$ values varied between −30.1 and −26.2‰ (average = −28.3‰) for the Oubangui River specimens, while values were slightly higher in specimens from the Niger River, ranging between −26.1 and −23.8‰ (average = −25.7‰).

4. DISCUSSION

To test if freshwater bivalve shells can be used as proxies for hydrologic variations in tropical rivers, we first verify if bivalve shell carbonate is precipitated in oxygen isotope equilibrium with the host water. Secondly, we test if $\delta^{18}O_w$ could be reliably reconstructed from $\delta^{18}O_{shell}$ values, and examined the influence of temperature variability on these estimates. Thirdly, the relationship between $\delta^{18}O_w$ and discharge was then used to assess whether reliable discharge estimates can be derived from $\delta^{18}O_{shell}$ data. Finally, we discuss the utility of $\delta^{13}C_{shell}$ data as a potential proxy for discharge and/or $\delta^{13}C_{DIC}$ values.

4.1. Observed versus calculated (model) shell $\delta^{18}O$ variations

Shell $\delta^{18}O$ values from both rivers exhibited sinusoidal patterns, with variations clearly reflecting the dry/wet seasons (Figs. 4 and 5). To examine if shell aragonite is precipitated in oxygen isotope equilibrium with the water, we applied Eqs. (1) and (2) to calculate predicted $\delta^{18}O_{shell}$ values, using measured $\delta^{18}O_w$ values and temperature (i.e., the model shell). To assign intra-annual dates to shell data, measured $\delta^{18}O_{shell}$ values were tuned to calculated model $\delta^{18}O_{shell}$ values using the date of collection as a starting point (see for example, Dettman et al., 1999; Kaandorp et al., 2003; Goewert et al., 2007). All shells per site were combined into a 'master shell' chronology using the intra-annual dates mentioned above. Shell oxygen isotope data matched modeled shell values well (Fig. 6A and B) demonstrating that these shells are good proxies of sub-seasonal environmental conditions.

The $\delta^{18}O_{shell}$ data from both rivers follow the seasonal patterns observed in $\delta^{18}O_w$ data (Figs. 2A and B). The range in predicted $\delta^{18}O_{shell}$ data, −5.2‰ to +0.7‰ for the Oubangui River (Fig. 4) and −6.3‰ and +4.5‰ for
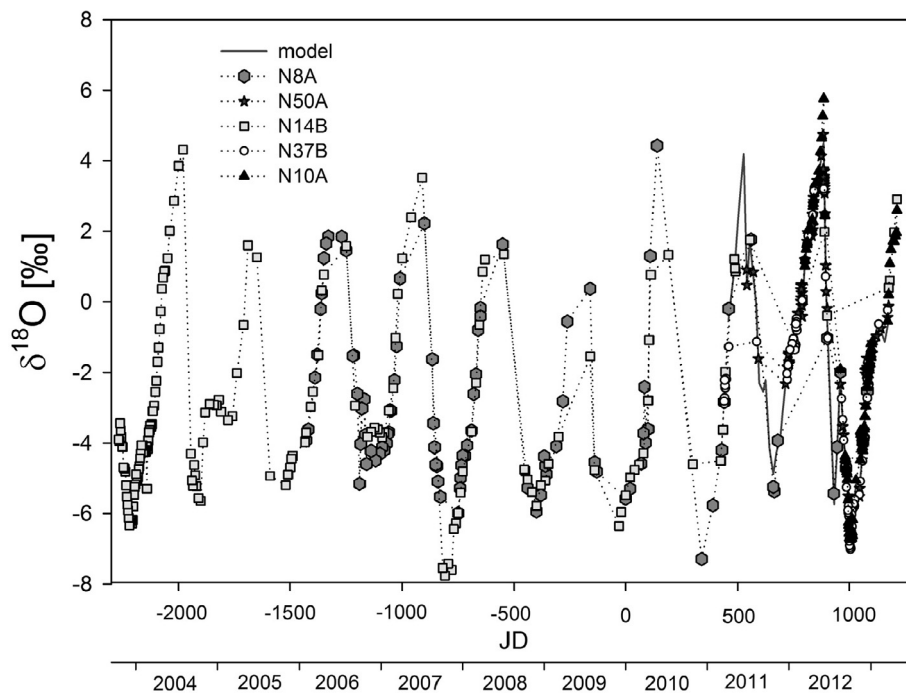

Fig. 5. Oxygen isotope records from five bivalves collected from the Niger River (various symbols representing different specimens: two *C. wissmanni* shells – squares and hexagons; two *A. dahomeyensis* – stars and circles; *A. chaiziana* – triangles), plotted with model shell (solid grey line). The primary *x*-axis represents the Julian date used for matching actual shell values with the model shell calculated from water data. Note that Julian dates below 500 are rough approximations because there was no model shell to match these samples with. The secondary *x*-axis is the calendar year spanning the lifetime of the oldest shell.

the Niger River (Fig. 5) agreed well with the measured δ^{18}O$_{shell}$ values over the entire dataset. This confirms that the analyzed shells precipitate their carbonate in oxygen isotope equilibrium with the surrounding water and cover most of the modeled shell data range as has been shown in previous studies on unionids (Dettman et al., 1999; Goewert et al., 2007). Considering that the patterns in the oxygen stable isotope record of all analyzed shells followed the seasonal cyclicity of δ^{18}O$_w$ of the host water, the age of the analyzed specimens was estimated by counting oxygen isotope cycles measured in the shells (cf. Elliot et al.,

2003; Ivany et al., 2003; Gillikin et al., 2005a,b; Versteegh et al., 2010; Goodwin et al., 2010, 2013).

Overall, δ^{18}O data of all shells follow the cyclicity of the δ^{18}O$_w$ data in both rivers, but shells with an ontogenetic age between 2 to 3 years best matched the full range of δ^{18}O values in model shells. For example, shells BB6 from the Oubangui and N10A from the Niger River grew for less than three years and show an exceptional match with modeled shell values (Fig. 6). However, when comparing the tuned δ^{18}O$_{shell}$ data with model δ^{18}O$_{shell}$ data, a number of growth gaps can be observed in several of the other shells
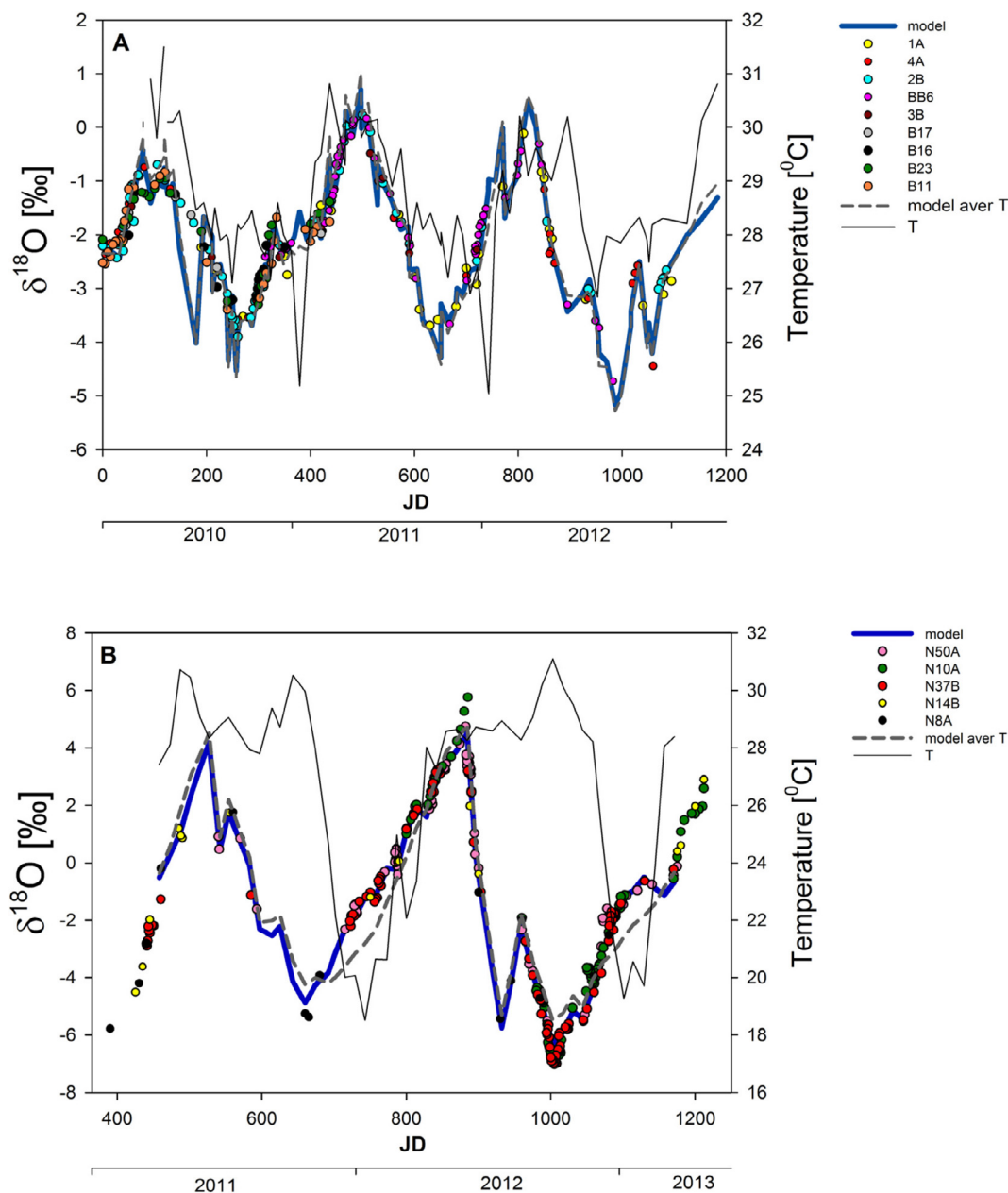

Fig. 6. Master shell δ^{18}O data from all shells (circles) analyzed from both sites plotted with model shell (solid line), where the time axis (x-axis; primary-Julian days (JD), secondary-years) covering the monitoring period for (A) the Oubangui River at Bangui between 2010 and 2012 and (B) the Niger River at Niamey during 2011 and 2012. Grey solid line is the water temperature, while dashed line represents the model shell values calculated with average temperature (to exclude temperature dependence).

(Figs. 4 and 5), illustrating that shell growth is non-linear and non-continuous over the bivalve's lifetime (cf. Goodwin et al., 2003). Freshwater mussel species from temperate rivers tend to reduce their growth, even to a stage of growth cessation below certain temperature levels; 12–17 °C was proposed as a threshold value by numerous authors (Dettman et al., 1999; Goewert et al., 2007; Versteegh et al., 2009). Growth cessation (or significantly reduced growth not being detected due to time–averaged samples) in our analyzed shells is likely not temperature related, although we found no data on threshold temperatures for tropical freshwater bivalve species, *in situ* temperatures did not drop below the aforementioned values. The lowest measured water temperatures were 18.5 °C (Niger River) and 25.1 °C (Oubangui River) (Fig. 3A and B) and specimens from both rivers grew under these temperature conditions (Fig. 6A and B). Therefore these gaps most likely result from unfavorable growth conditions, such as high turbidity, or low water levels (e.g., causing temporary aerial exposure). We hypothesize that several shells temporarily shut down during high discharge events because of high turbidity. Total suspended matter concentrations (TSM) increase during high discharge peaks in the Oubangui River (data presented in Bouillon et al., 2014), which represents an unfavorable growth condition for bivalves (Kryger and Riisgård, 1988; Kaandorp et al., 2003). Oubangui shells B23 and B11 stopped/reduced growing for about 150 days during 2010 (Fig. S11, supplementary material) and shell 3B shows a growth cessation of about 130 days in 2011, both during periods of high discharge. In contrast, growth gaps in the shells from the Niger River are mainly recorded during low water conditions (Fig. 5). Aerial exposure of these shells could offer an explanation for a growth gap (125 days) in shell N37B, a young bivalve, which is expected to grow rapidly and continuously. There have been reports that a species of *Aspatharia* in Lake Malawi (East Africa) aestivating in the dry mud at the level of last floodwater throughout the dry season, moreover, anecdotal reports suggest they can survive under desiccated conditions for more than two years and revive within half an hour when immersed in water (Beadle, 1974). In addition, temperate mussels have been shown to slow growth significantly over a 14-year period (to less than 300 μm yr^{-1}; Kesler et al., 2007). In the analyzed shells, gaps were found throughout the shells, but were mostly in ontogenetically older shell sections, when the bivalve does not invest as much energy into shell growth (Goodwin et al., 2003). Thus, shell growth can also be affected by ontogenetic age.

Freshwater mussel species used in our study are not well represented in the literature, to the best of our knowledge there is no information about growth patterns or burying preferences for these species. Sectioned shells did not show clear evidence of systematic internal growth lines, nor were internal growth lines comparable with external growth lines (see Haag and Commens-Carson (2008) for a discussion on unionid growth lines). Only a single shell from each of the two sampling sites exhibited clearly distinguishable growth lines in shell sections that were concurrent with external lines. In shell (3B) from the Oubangui River each growth line corresponded to a negative peak in the $\delta^{18}O_{shell}$ record.

The shell from the Niger River (N14B) showed an opposite behaviour, with the growth lines corresponding to positive peaks in the $\delta^{18}O_{shell}$ record. Growth lines have been shown to be related to growth cessation due to environmental conditions (e.g., Goewert et al., 2007; Haag and Commens-Carson, 2008; Versteegh et al., 2010). This supports our hypothesis that bivalves from Oubangui River have limited tolerance for high discharge, thus they grow until the conditions are suitable for carbonate precipitation, then after a shorter or longer growth cessation (or extremely reduced growth) they restart shell production, forming a new layer when the conditions are appropriate again (during moderate discharge). Bivalves from the Niger River are prone to aerial exposure due to very low water level during the dry season. The positive $\delta^{18}O_{shell}$ peaks measured in samples near growth lines suggest that those specimens grew while there is a sufficient water flow, but stopped at low flow when $\delta^{18}O_w$ values were high. This hypothesis is also supported by the missing high $\delta^{18}O_{shell}$ values in the shells from Niger River.

Other authors have expressed the benefits of using younger bivalves for sclerochronological studies, because of the high growth rate in the first few years of life (e.g., Chauvaud et al., 2005), but due to water flow and bivalve movement, shell erosion may remove the first months or year of shell growth in freshwater bivalves (Kesler and Bailey, 1993). In the later stage of ontogeny, shell growth is reduced, which results in narrower growth increments and more compressed $\delta^{18}O_{shell}$ cycles toward the ventral margin. Narrower increments cover more time in each drill sample, thus more time is averaged in each sample (Goodwin et al., 2003). For example, the highest sampling resolution per calendar year was achieved in the juvenile part of shell 3B (101 samples in one year of growth with 350 μm sampling distance, which represents an average shell growth rate of 96 μm per day), while in the same shell, through ontogeny, the growth increment widths decreased, and in the eighth year only 13 samples were drilled with the same sampling resolution. The latter equates to an average growth rate of 12 μm per day, thus each 350 μm wide drill hole averages 29 days of growth. In these shell regions, short-term extreme environmental conditions will most likely not be detected and the annual $\delta^{18}O_{shell}$ amplitude may decrease (see Goodwin et al., 2003). Indeed, longer-lived shells show ontogenetic decreases in amplitude as they age. For example, shell B17, an eight-year-old individual, shows a clear decrease in amplitude of $\delta^{18}O_{shell}$ values though life (Fig. 4), with a reduction in range of over 1‰ (from 2.8‰ to 1.4‰) in the seventh growth year.

Calculating with different models, Versteegh et al. (2010) demonstrated that the growth of unionids from temperate rivers is nonlinear, and is dependent on temperature and food availability. Kaandorp et al. (2003) measured growth rates of up to 0.5 mm day^{-1} in the early life stage of an *Anodontites trapesialis* from an Amazonian floodplain lake. Based on matching $\delta^{18}O_{shell}$ values with predicted $\delta^{18}O_{shell}$ values, daily growth rates of our analyzed shells (see Figs. S6 and S7, supplementary material) were between 0.002 and 0.75 mm day^{-1} (Oubangui River) and 0.002–0.7 mm day^{-1} (Niger River). Unlike the unionids

from temperate rivers, growth changes in our shells showed no distinct seasonality but were more age-dependent, i.e., high growth rate in the early life stages and decreasing annual growth rate at the later stage (Figs. S6 and S7; supplementary material).

In the Niger River, all shells were collected in 2013 and were either ontogenetically young (∼2 years) or older (∼9 years). Therefore, shell data matched the full range of modeled data over the last ∼2 years, which was well represented by these fast growing young bivalves (monitoring years 2 and 3). However, the first year of water monitoring was not well represented by shell data (Fig. 6B) because of time averaging effects, with the first year of water monitoring (2011) represented only by shells in their 7th year of life.

In addition to environmental conditions and ontogenetic effects leading to shell growth reduction or cessation, some individual differences are also evident. For example, three *C. wissmanni* (1A, 2B and 4A) collected in March 2013 from the Oubangui were found to have a similar ontogenetic age, but do not show the same range of $\delta^{18}O_{shell}$ values. Two shells (2B and 4A) track the high $\delta^{18}O_{shell}$ values in the first year of monitoring, while the high values in the second year of monitoring are recorded only by shell 2B, whereas the other two experienced slower growth and did not record this time period (Fig. 7). Nevertheless, the data from the 14 shells from both river systems illustrate that when several shells of various ontogenetic age are combined, there is a higher probability of covering the full range of environmental conditions. Therefore, to circumvent problems of growth hiatuses, it is recommended to use several shells of varying ontogenetic age to build a master shell chronology, which has a higher probability of capturing the full range of environmental conditions.

There have been some reports of species-specific oxygen isotope fractionation in mollusks. For example, Mueller-Lupp et al. (2003) determined a −0.37‰ offset between expected and measured $\delta^{18}O$ in *Astarte borealis*, Yan et al. (2012) almost a 2‰ offset in the shallow-marine bivalve, *Eurhomalea exalbida*. However, these studies are somewhat dubious in that the monitoring station collecting environmental data was not adjacent to the shell collection site. Most studies have shown that bivalves closely match oxygen isotope equilibrium and this is also the case for unionid bivalves (Dettman et al., 1999; Goewert et al., 2007) and land snails (Zanchetta et al., 2005). In our study, we analyzed 14 bivalves representing three different species (Table 1), and found no evidence for species-specific oxygen isotope fractionation. Bivalves from the Niger River belong to three different species, but all specimens followed the pattern of the model shell. Although longer-lived specimens of *C. wissmanni* (N8A and N14B) exhibited numerous gaps in the ontogenetically older shell sections, they still reliably follow $\delta^{18}O_w$ values. Juvenile specimens of *A. chaiziana* (N10A) and *A. dahomeyensis* (N37B and N50A) matched the modeled shell and each other exceptionally well. Given that the nine analyzed bivalves from the Oubangui River belong to the same species (*C. wissmanni*), there were no species-specific issues relating to this dataset.

As previously noted, water temperature and $\delta^{18}O_w$ values are expected to control $\delta^{18}O_{shell}$ values (Dettman et al., 1999). As can be seen in Fig. 6A and B, measured $\delta^{18}O_{shell}$ values were synchronized with the model shell $\delta^{18}O$ record (calculated with measured temperatures). To visualize the effect of temperature on shell oxygen isotopes, we also calculated a model shell $\delta^{18}O$ record using average
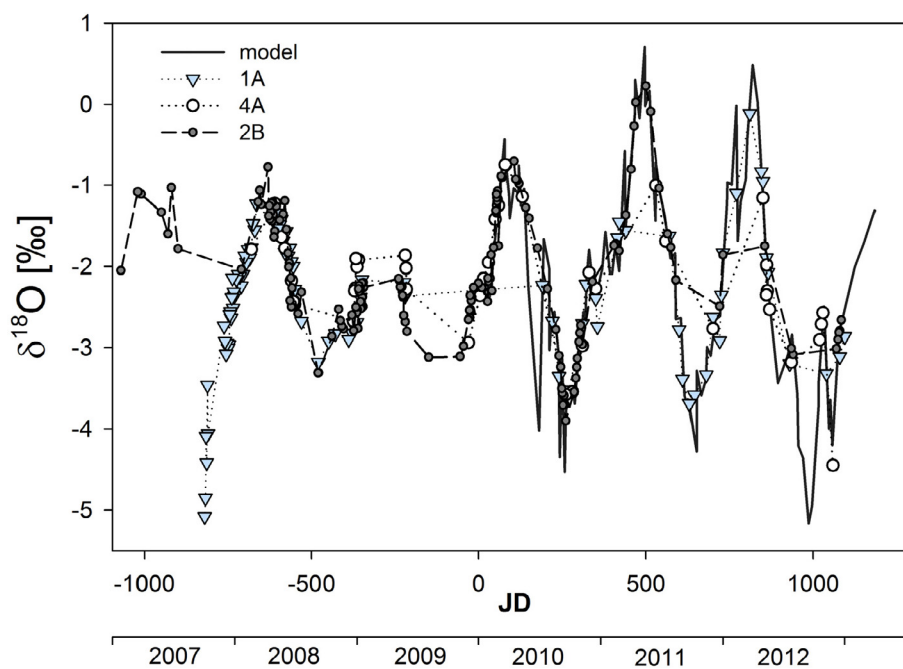

Fig. 7. $\delta^{18}O$ data from three bivalve shells (each represented by a single symbol) collected in 2013 from Oubangui River, aligned with the model shell (solid line) (see text). X-axis follows Fig. 6.

water temperature data (see Fig. 6A and B). Temperature in both rivers was close to the average value for most of the year. Thus, the two model shells match one another for most of the time period, but observable discrepancies occurred during relatively colder times, when $\delta^{18}O_{shell}$ values slightly shift towards higher values, even though $\delta^{18}O_w$ remained

nearly unchanged. As temperature in the Oubangui River deviated only slightly from the average values over the entire year, deviations between the two model $\delta^{18}O_{shell}$ records are hardly recognizable (Fig. 6A). The larger temperature range and longer duration of a 'cool' period in the Niger River affected the $\delta^{18}O_{shell}$ record more visibly, causing a higher
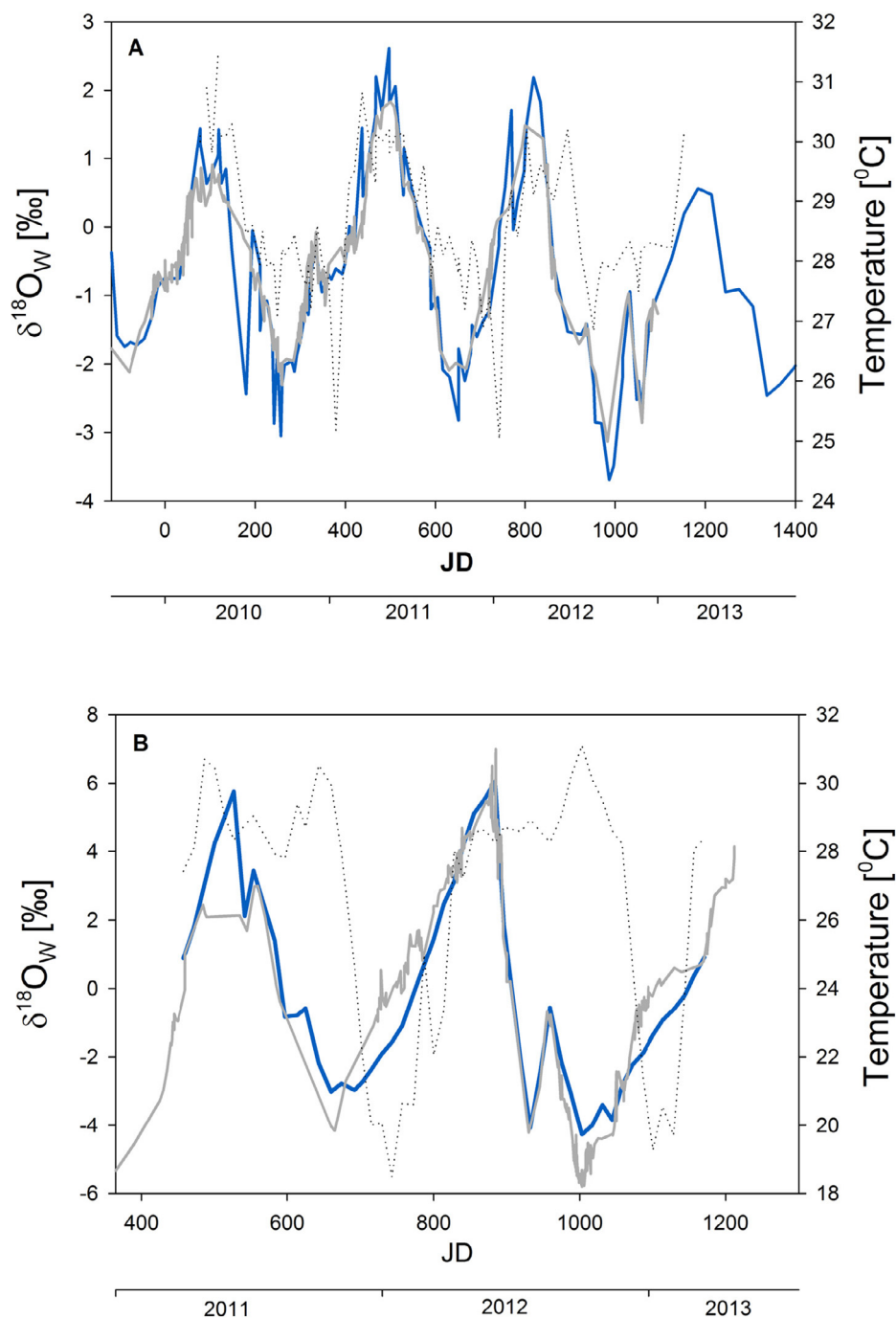

Fig. 8. Measured $\delta^{18}O_w$ values (solid blue line) from both sites plotted with reconstructed $\delta^{18}O_w$ values (solid grey line) calculated from master shell $\delta^{18}O$ values using average temperatures, where the time axis (x-axis; primary-Julian days (JD), secondary-years) covering the monitoring period for (A) the Oubangui River at Bangui between 2009 and 2013 (together with the additional available $\delta^{18}O_w$ data from the GNIR database) and (B) the Niger River at Niamey during 2011 and 2012. Dotted line is the measured water temperature. (For interpretation of the references to colour in this figure legend, the reader is referred to the web version of this article.)
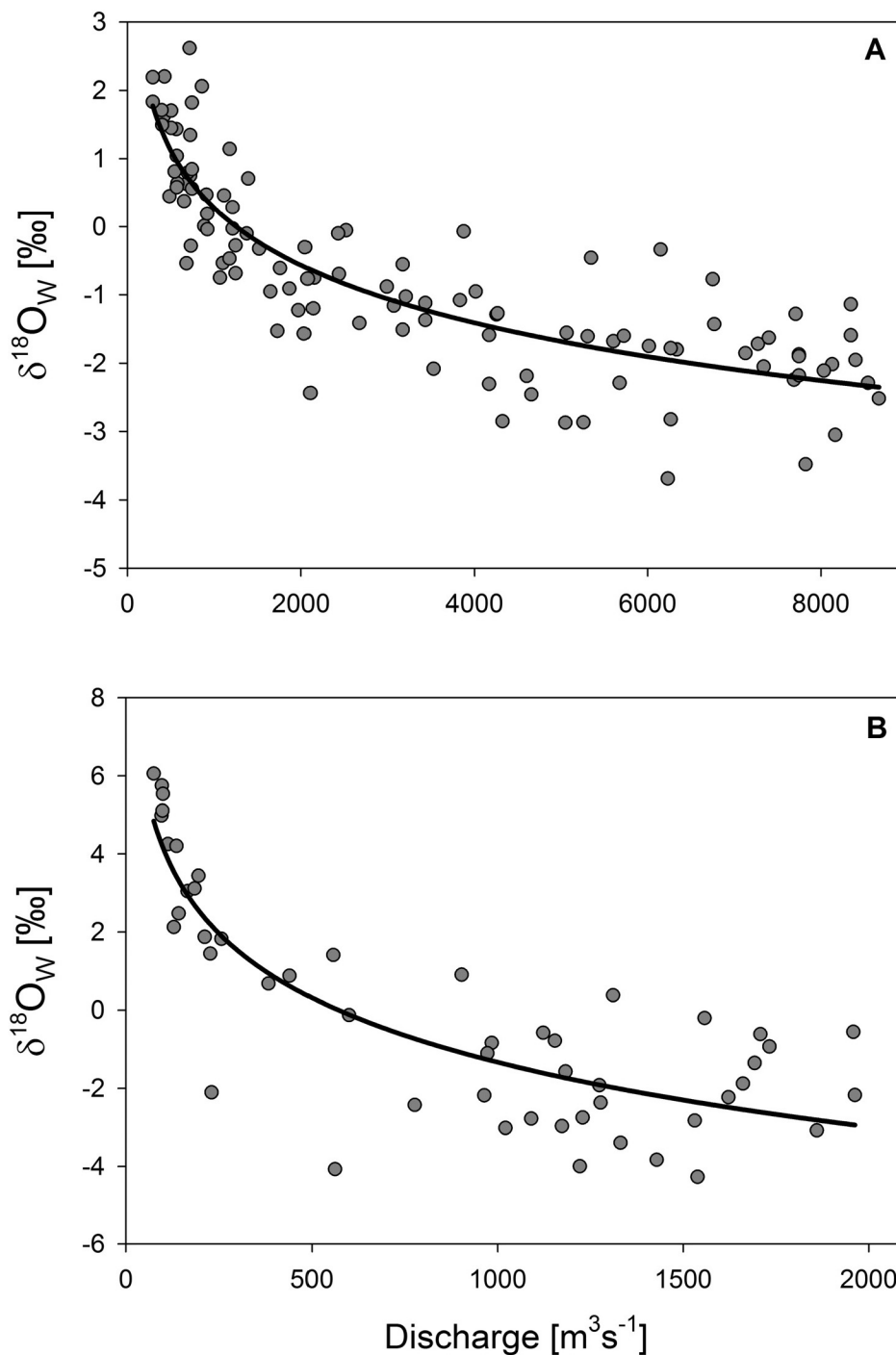
Fig. 9. Correlation between discharge and $\delta^{18}O_w$ values for (A) the Oubangui River at Bangui, and (B) the Niger River at Niamey. Regression relationships are: $\delta^{18}O_w = -1.222\ln(Q) + 8.741$ ($R^2 = 0.75$) for the Oubangui, and $\delta^{18}O_w = -2.383\ln(Q) + 15.128$ ($R^2 = 0.75$) for the Niger.

deviation from the expected values if only average temperature values were considered (Fig. 6B).

4.2. Reconstructing water $\delta^{18}O$ values from shell $\delta^{18}O$ values

At our study sites, water temperature variations play a relatively small role in $\delta^{18}O_{shell}$ values (1‰ change in $\delta^{18}O_{shell}$ per ~4.7 °C; Grossmann and Ku, 1986), compared to the seasonal amplitude in $\delta^{18}O_w$ values. To test if bivalves can be used to reconstruct $\delta^{18}O_w$ values, we calculated $\delta^{18}O_w$ values from $\delta^{18}O_{shell}$ values using average water temperature and Eqs. (1) and (2). Average temperature should be somewhat predictable back ~100 years in tropical Africa and change little (less than 1 °C; Hulme et al., 2001). Moreover, based on Eqs. (1) and (2), a 1 °C difference in water temperature leads to a rather

small (0.19‰) change in calculated $\delta^{18}O_w$ values. Average temperature values for the monitoring period were 28.6 ± 1.2 °C in the Oubangui River and 26.6 ± 3.7 °C in the Niger River. Shell data from earlier than the temperature monitoring period (which is shorter than the $\delta^{18}O_w$ record) were aligned with measured $\delta^{18}O_w$ values using the method described in Section 2.3. For the $\delta^{18}O_w$ reconstruction, the aligned 'master shell' (Fig. 6A and B) was used, since multiple shells merged into one provides more continuous data points than when using just a single shell. The other advantage of using a master shell is that combining young bivalves with older
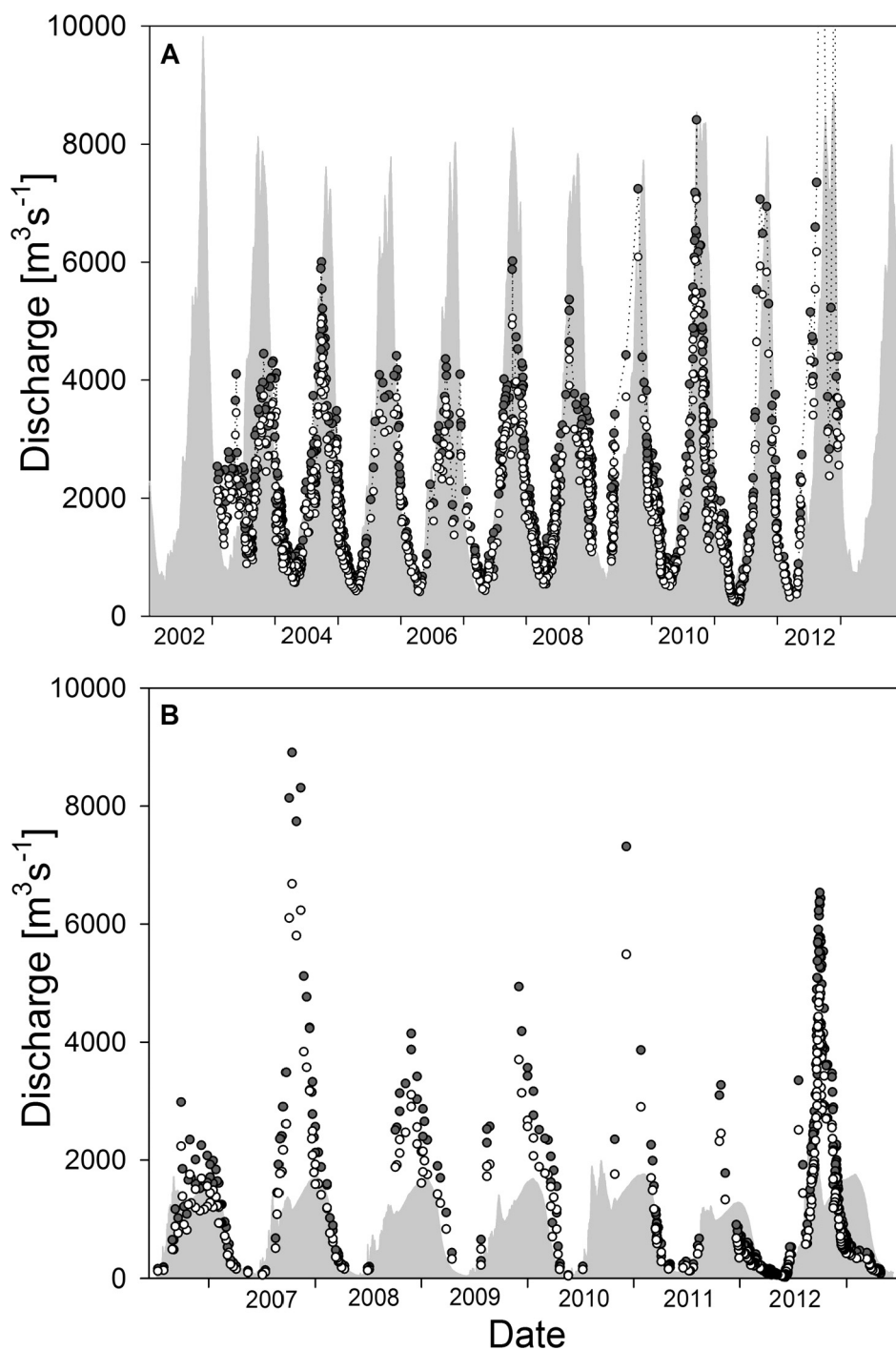

Fig. 10. Comparison of measured daily discharge data (grey-shaded area) of the (A) Oubangui River at Bangui for the period 2002–2013 and reconstructed discharge values using average temperature of 28.6 °C (black circles) or using 1 standard deviation elevated temperature of 29.7 °C (open circles) and (B) Niger River at Niamey for the period 2002–2013 and reconstructed discharge values using average temperature of 26.6 °C (black circles) or using 1 standard deviation elevated temperature of 30.3 °C (open circles).

ones, results in a finer sampling resolution over the entire dataset and circumvents time-averaging. The calculated $\delta^{18}O_w$ values from the master shell fit well with the corresponding water data, which ranged between -3.5 and $+1.8‰$ and between -6.5 and $+7‰$ for the Oubangui and Niger River, respectively, for the entire period covered by the analyzed bivalves (Fig. 8A and B).

Being located in (sub)tropical regions, both rivers exhibit a relatively predictable temperature range. Cooler periods in both rivers occur around January and last for about a month at Bangui, while at Niamey the temperature can stay lower until February or March, but the concomitant decrease is not seen in measured $\delta^{18}O_w$ values. Although reconstructed $\delta^{18}O_w$ values are affected, and slightly shift towards higher values (because average temperature is used for $\delta^{18}O_w$ reconstruction), the difference is minimal and very closely approximates the measured $\delta^{18}O_w$ values. Departure from measured $\delta^{18}O_w$ values in the Oubangui River is visible during January, but due to the short duration and small temperature range, the difference is slight (less than $0.5‰$). In the Niger River, the cooler water accompanies the second discharge peak, and lasts several months, which is clearly distinguishable in the shell $\delta^{18}O$ record, and thus in the reconstructed $\delta^{18}O_w$ values as well. Although, a positive shift in reconstructed $\delta^{18}O_w$ values appears (up to $1.7‰$) during those months, the remainder of the reconstructed data closely follows the measured values. Therefore, the $\delta^{18}O_w$ reconstruction is reliable, even in a complex system such as the Niger River.

To estimate the sensitivity of $\delta^{18}O_w$ reconstruction, calculations were also made using an average temperature ± 1 standard deviation relative to the observed mean. This resulted in a positive offset using higher temperatures and in a negative offset using lower temperatures ($\pm 0.2‰$ in the Oubangui River and $\pm 0.7‰$ in the Niger River) in reconstructed values. The Niger River has a larger temperature range ($13\,°C$) than the Oubangui River ($6\,°C$), which is the main reason for the larger offset in the Niger data. Nevertheless, these differences are small compared to the annual range in $\delta^{18}O_w$ values, which ranges more than $5‰$ at each site (Fig. 2A and B). Temperature sensitivity is, however, of importance for any attempt at paleoclimate reconstruction. Different temperature zones react with different sensitivity. According to Hulme et al. (2001), the average annual temperature increase in Africa was about $0.5\,°C$ during the 20th century. Such an increase is negligible considering the temperature sensitivity discussed above. Thus, these data suggest unionid $\delta^{18}O_{shell}$ values can provide a good estimate of $\delta^{18}O_w$ values across tropical Africa, thereby providing insight into past hydroclimate.

4.3. Relationships between discharge and $\delta^{18}O_w$

Discharge (Q) seasonality in both river systems is mirrored by $\delta^{18}O_w$ variations (Fig. 2A and B), and the resulting relationships between daily discharge and concomitant $\delta^{18}O_w$ data were best described by logarithmic equations (Fig. 9):

$$\text{For the Oubangui}: \delta^{18}O_w = -1.222\ln(Q) + 8.741$$
$$(R^2 = 0.75, n = 112) \qquad (3)$$

$$\text{For the Niger}: \delta^{18}O_w = -2.383\ln(Q) + 15.128$$
$$(R^2 = 0.75, n = 50) \qquad (4)$$

The nature of this inverse relationship between Q and $\delta^{18}O_w$ values puts certain constraints on the possibilities for discharge reconstructions based on $\delta^{18}O_w$ values estimated from $\delta^{18}O_{shell}$ variations. Since $\delta^{18}O_w$ values change little between average and high discharge conditions, and the relationship shows large scatter in the data in this region, reconstruction is difficult during periods of high discharge (see Fig. 9). In contrast, $\delta^{18}O_w$ values show a wide range with less variability in the region of lower Q, and we can thus expect reconstructed $\delta^{18}O_w$ values to allow Q estimations during low discharge events.

A small time shift (approximately 30 days) is observed between $\delta^{18}O_w$ values and peak discharge in the Oubangui (Fig. 2A). In particular, $\delta^{18}O_w$ values start to decrease slightly earlier than discharge starts to rise, they then reach their maximum and minimum at approximately the same time. Conversely, the falling limb of the hydrograph is followed with a slight delay of $\delta^{18}O_w$ values, until they both reach the minimum and maximum values at approximately the same time. We propose that this could be caused by abundant precipitation in the area, whereby local ^{18}O-depleted rainfall is entering the river faster than the discharge peak arrives from further upstream in the catchment. Unfortunately, precipitation $\delta^{18}O$ data from the Oubangui basin is not available except for at Bangui itself, which is unlikely to reflect the signature of average watershed precipitation considering the large area of the catchment upstream of our sampling site. The low $\delta^{18}O_w$ values during the wet season are expected to reflect ^{18}O-depleted precipitation, as the main contributor to discharge is an influx from direct runoff during this season. After the dry season, the Oubangui River becomes ^{18}O-enriched because of increased evaporation due to the increased water residence time, higher temperatures and lower humidity, and due to the larger contribution of groundwater to the river flow. Stroppiana et al. (2011) demonstrated that for the Uele River (an important tributary in the upper catchment, which forms the Oubangui River after its confluence with the Mbomou River) the highest discharge typically occurs a few months following the main rainfall peaks, largely due to the interception and evapotranspiration of rainfall by the forest canopy.

Given that the Niger River has a two-peak hydrograph, the relationship between $\delta^{18}O_w$ and discharge is somewhat more complex than in the Oubangui, even if the relationship also fits a logarithmic trend with a similar R^2 value (Fig. 9). In the Niger River the two discharge peaks originate from different water sources, which likely have different $\delta^{18}O_w$ signatures. In support of this, there is a small increase in $\delta^{18}O_w$ values coinciding with peak discharge of the first (local) flood. However, during the second flood, the $\delta^{18}O_w$ values increased gradually, reaching their maximum months later at the time of the lowest discharge (in both years of monitoring). The first discharge peak at

Niamey in August–September results from water arriving via small local rivers originating from heavy rains during the wet season. At this time, about 30 temporary streams (koris) are contributing to river discharge, because soil degradation in Niamey area in the past ~20 years has led to conversion of endorheic basins into exorheic basins, which now flow directly into the Niger River (Amogu et al., 2010). These koris are usually very shallow, thus the first water load is usually more ^{18}O-enriched due to the high evaporation during the dry season. Therefore, it is this ^{18}O-enriched water from the koris that cause the small increase in $\delta^{18}O_w$ values during the first flood.

These two (sub)tropical rivers express a strong seasonality, distinguishing clearly by the wet and dry season. The ratio of Qmax/Qmin is nearly 20 for both river systems, which is reflected in the large amplitude of $\delta^{18}O_w$ values. In some other African tropical river systems, the difference between low and high flow discharge is much lower, and hence the oxygen isotope variability is expected to be less pronounced. For example, the mainstem of the Congo River at Kinshasa has a Qmax/Qmin ratio of 2–2.5, with $\delta^{18}O_w$ values between −0.2 and −3.1‰ (data deposited and publicly available through the GNIR database: http://www-naweb.iaea.org/napc/ih/IHS_resources_isohis.html). A smaller Qmax/Qmin ratio results in less pronounced seasonality, mainly because the effects of dry and wet seasons are smoothed out with a nearly constant water load.

4.4. Reconstructing river discharge based on shell $\delta^{18}O$ data: potential and limitations

As described in Section 4.2, we first calculated $\delta^{18}O_w$ from the master shell $\delta^{18}O$ data, then reconstructed discharge using Eqs. (3) and (4). Due to the logarithmic relationship, this reconstruction has some limitations, and is mainly applicable for low discharge reconstructions. A comparable study of discharge reconstruction from freshwater bivalve $\delta^{18}O_{shell}$ data by Versteegh et al. (2011) in the temperate river Meuse came to a similar conclusion, being that due to the logarithmic relationship between discharge and $\delta^{18}O_w$ values, quantitative discharge reconstruction is only possible during low flow and by analyzing a large number of samples.

To conduct an error analysis based on the assumption of average temperature (as would be done with older shells), we tested the effect of temperature on calculated discharge. As described above, we used an average temperature for $\delta^{18}O_w$ reconstruction instead of measured biweekly values, since we wish to examine the potential of this proxy for sites or time periods without *in situ* temperature data. Subsequently, we recalculated $\delta^{18}O_w$ using temperature with ±1 standard deviation. As a first approach, the calculation using average temperature resulted in a reliable fit with the low discharge periods, but high discharge was either highly over- or underestimated (Fig. 10). The lowest $\delta^{18}O$ values recorded in shells (and calculated $\delta^{18}O_w$), resulted in unrealistically high discharge calculations due to the logarithmic relationship

between Q and $\delta^{18}O_w$ values. Furthermore, the timing between the actual and calculated discharge is not always accurate because of the observed time shift between the discharge events and $\delta^{18}O_w$ values, therefore the calculated discharge peak appears earlier. However, despite the time shift, the low discharge values agree very well (Fig. 10A). Secondly, to test the temperature sensitivity in the Oubangui River, discharge was calculated using temperature one standard deviation higher (+1.2 °C) than the average (29.7 °C). This resulted in overall 16% lower reconstructed discharge values. Further, using temperature of 27.3 °C (one standard deviation lower) the reconstructed discharge was 21% higher over the entire dataset. Thus, the sensitivity for reduced temperatures was more accentuated than for higher temperature estimates.

Reconstructing discharge of the Niger River resulted in a similar outcome to the Oubangui shells: low discharge events calculated nearly correctly, while high discharge was highly overestimated (Fig. 10B). Using an average temperature of 26.6 °C, the reconstructed $\delta^{18}O_w$ data missed the most negative values, which were directly related to high discharge. Although the most negative $\delta^{18}O_w$ values are "smoothed out" with average temperature, the high amplitude of $\delta^{18}O_w$ values and the logarithmic relationship between discharge and $\delta^{18}O_w$ values caused the large exaggeration of high flow discharge calculations. The temperature sensitivity in the Niger River is somewhat more pronounced than in the Oubangui River, as calculations with 1 s.d. lower temperature (i.e. 3.7 °C) resulted in 35% higher discharge, while using 1 s.d. higher temperature resulted in a 25% lower discharge.

Dettman et al. (2004) pointed out that freshwater bivalves are very sensitive to suspended sediment load, and likely cease growth during high discharge events. This seems applicable to the Oubangui shells as well, since discharge values over 5000 m³ s⁻¹ were rarely reconstructed from shell data (Fig. 10A). The exception was with records from young continuously growing shells, which grow despite unfavorable conditions. Therefore, discharge was fully recorded in the years between 2009 and 2012 by the young specimens collected between 2011 and 2013. Gaps were noted in discharge reconstructed from ontogenetically older bivalves, which are more sensitive to environmental changes. Thus, this suggests that shells from Oubangui River experience a temporary shutdown in growth when the river discharge reaches a threshold value, possibly due to increased turbidity (bed load).

While the shell data could be used to reliably reconstruct discharge during low flow conditions over the entire record of the 'master shell' in the Oubangui River, this was only possible for the last year in the Niger River as this was the only period covered at sufficiently high resolution by young shells. Older bivalve specimens appear not to record environmental conditions during low discharge periods, which may suggest growth shutdown during low water levels when the shells living in the Niger River could be exposed to air. Overall, bivalve shells from both sites were found to have a high potential to reconstruct discharge patterns, but high discharge conditions were difficult to capture due to growth cessation (as suggested for the Oubangui

River) and due to the logarithmic relationship between Q and $\delta^{18}O_w$.

4.5. Relationships between discharge and $\delta^{13}C_{DIC}$

Strong seasonality was observed in $\delta^{13}C_{DIC}$ values in both the Oubangui and Niger River. In the Oubangui River, changes in $\delta^{13}C_{DIC}$ values co-varied with changes in $\delta^{18}O_w$ values (Fig. 2A) and have a strong linear relationship ($R^2 = 0.72$). Variations in $\delta^{13}C_{DIC}$ values in river systems are known to be a result of a range of different processes, including changes in the importance of silicate and carbonate weathering (linked to the main water sources supplying the river discharge, i.e. groundwater versus surface runoff), and seasonality of *in situ* primary production and mineralization (Probst et al., 1994; Bullen and Kendall, 1998; Bouillon et al., 2012). For the Oubangui River, the more ^{13}C-depleted values during high discharge conditions have been linked to an increased relative importance of silicate weathering, while during low discharge, *in situ* production by phytoplankton production is thought to leave the DIC pool more enriched in ^{13}C (Bouillon et al., 2012, 2014).

In the Niger River the highest $\delta^{13}C_{DIC}$ values ($-1.8‰$) were measured at the falling limb of the second discharge peak (Fig. 2B). A similar pattern to that observed in $\delta^{18}O_w$ values (see Section 4.3) can be discerned: at the time of the first flood, $\delta^{13}C_{DIC}$ values slightly increase simultaneously with arrival of the discharge peak, while with the second flood, the $\delta^{13}C_{DIC}$ peak is delayed – increasing immediately after the discharge peak. After reaching the peak values of about $-2‰$, $\delta^{13}C_{DIC}$ values start to rapidly decrease to reach the minimum concomitant with $\delta^{18}O_w$ values. At the time of the rainy season, the water transported in the Niger River is mainly coming from three Sahelian tributaries (Gorouol, Dargol, and Sirba), which are temporary rivers, transporting water with a high suspended sediment load arising from erosion of the local soil (Descroix et al., 2012). Unlike in the Oubangui River, the co-variation between $\delta^{18}O_w$ and $\delta^{13}C_{DIC}$ in the Niger River was not clear, likely due to the time shift between these two parameters.

4.6. Controls on shell $\delta^{13}C$ signatures: environmental versus vital effects

While the main focus of our study was on validating the use of $\delta^{18}O_{shell}$ data to reconstruct $\delta^{18}O_w$ values and discharge, it is worth examining the $\delta^{13}C_{shell}$ data and the relationship with $\delta^{13}C_{DIC}$ values, in particular since the latter also show an excellent correlation with discharge in the Oubangui River (Fig. 2A). $\delta^{13}C$ values of shells are mainly controlled by $\delta^{13}C_{DIC}$ values (reviewed in McConnaughey and Gillikin, 2008). However, as many authors suggested, metabolic carbon is also a major contributor to shell carbon (Lorrain et al., 2004; Gillikin et al., 2007, 2009; McConnaughey and Gillikin, 2008). We estimated the metabolic carbon contribution to the shell (C_M) by applying a simple mixing model (see also McConnaughey et al., 1997):

$$C_M = \frac{\delta^{13}C_{shell} - \varepsilon - \delta^{13}C_{DIC}}{\delta^{13}C_M - \delta^{13}C_{DIC}} \qquad (5)$$

using a fractionation factor (ε) between aragonite and bicarbonate of $+2.7‰$ (Romanek et al., 1992). Following McConnaughey et al. (1997), we approximated the metabolic carbon isotope value ($\delta^{13}C_M$) using soft tissue $\delta^{13}C$ values (measured in individual mantle or muscle tissues). For $\delta^{13}C_{shell}$ values, we used averages of the data across a growth period of an individual, while $\delta^{13}C_{DIC}$ values represent the average of the measured values during the monitoring period; hence the estimated C_M should be considered average values and do not reflect possible seasonal or ontogenetic variability. C_M estimates ranged between 7 and 18% in shells from the Oubangui River, but were higher (23–27%) in shells from the Niger River. Lorrain et al. (2004) suggested that young bivalves grow faster and mainly use carbon from the DIC pool of the host water for shell precipitation, while older bivalves reduce their shell growth and incorporate relatively more metabolic carbon into shell carbonate. Metabolic carbon is typically more ^{12}C-enriched in comparison to DIC, thus a higher contribution of metabolic carbon would correspond to a decrease in $\delta^{13}C_{shell}$ values. Unlike the freshwater mussels in Gillikin et al. (2009), in our study no clear pattern common to all specimens was observed between the ontogenetic age of the bivalves and the amount of metabolic carbon incorporation. While some of the shells in our study showed a clear decrease in $\delta^{13}C_{shell}$ values with age (e.g., shells 1A, 2B, and 4A from the Oubangui; shells N10A, N37B from the Niger, see Figs. S4 and S5, supplementary material), such a pattern of increasing C_M (decreasing $\delta^{13}C_{shell}$ values) was not observed in all specimens. Therefore, it does not seem this is a universal phenomenon in freshwater mussel shells. Furthermore, the seasonality of $\delta^{13}C_{shell}$ values did not closely match that observed in $\delta^{13}C_{DIC}$ values, suggesting $\delta^{13}C_{shell}$ data are not a good environmental proxy.

Goewert et al. (2007) suggested that $\delta^{13}C_{shell}$ values can be related to watershed characteristics, and could be used e.g. to distinguish vegetation types within river basins. While we found no evidence that $\delta^{13}C_{shell}$ data reliably track the seasonality in $\delta^{13}C_{DIC}$ values (Figs. S8–S10, supplementary material), the average and ranges in $\delta^{13}C_{shell}$ values were clearly different between the two river systems (Table 2), and could be related to average $\delta^{13}C_{DIC}$ values of both rivers. Thus, $\delta^{13}C_{shell}$ data do appear to have the potential to distinguish larger-scale differences in $\delta^{13}C_{DIC}$, which can in turn be linked to e.g. weathering regimes and catchment vegetation cover (e.g. Mook and Tan, 1991) The higher average $\delta^{13}C_{shell}$ values in the Niger River thus likely reflect the stronger contribution from C4 vegetation (increase in millet crops) in the Niger catchment (d'Herbè and Valentin, 1997; Leblanc et al., 2008), while lower $\delta^{13}C$ values of DIC and shell from Oubangui River are consistent with the higher forest cover (C3 vegetation) and the importance of silicate weathering (Bouillon et al., 2012, 2014).

4.7. Conclusions and outlook

Results from this study have shown that freshwater bivalves from the Oubangui and Niger Rivers precipitate shell aragonite in oxygen isotopic equilibrium with the host water. Due to low water temperature variations, these bivalves thus record seasonal $\delta^{18}O_w$ variations at high temporal resolution, in particular during the early life stages when high growth rates are observed. When comparing model $\delta^{18}O_{shell}$ data, calculated from measured river temperature and $\delta^{18}O_w$ values, with measured $\delta^{18}O_{shell}$ data, gaps in growth as well as nonlinear growth became apparent. Cessations in growth appear to be linked to different factors in the two river systems, occurring more during high discharge and high turbidity periods in the Oubangui River, but more prevalent during low water conditions and possible air exposure in the Niger River.

Using multiple shells merged into a master shell instead of single specimen, provided more continuous data and finer sampling resolution, thus more detailed $\delta^{18}O_w$ reconstruction. Reconstructions with average temperature for these (sub)tropical rivers was shown to be robust, as these reconstructions were relatively insensitive to the uncertainty in water temperatures (temperature sensitivity is 0.19‰ per 1 °C) in comparison with a high annual range of $\delta^{18}O_w$ values.

In both river systems studied, a logarithmic relationship was observed between $\delta^{18}O_w$ and river discharge, although such relationships are likely to be very system-specific and are not ubiquitous. Using these relationships to reconstruct river discharge demonstrated that mainly low discharge conditions could be reconstructed.

Establishing a model which uses freshwater bivalve shell $\delta^{18}O$ data as a proxy for river $\delta^{18}O_w$ reconstruction opens up the path to studying this proxy in archived museum specimens to determine changes in tropical river systems and their catchments (e.g., precipitation-evaporation budgets) over the past century. We anticipate that a range of additional proxies (e.g., $\delta^{15}N$, δD, element ratios, see O'Donnell et al., 2003; Carroll et al., 2006; Kaandorp et al., 2006) could broaden the possibilities of reconstructing riverine biogeochemistry and hydrological conditions.

APPENDIX A. SUPPLEMENTARY MATERIAL

Supplementary data associated with this article can be found, in the online version, at http://dx.doi.org/10.1016/j.gca.2017.03.025.

REFERENCES

Abell P. I., Amegashitsi L. and Ochumba P. B. O. (1996) The shells of *Etheria elliptica* as records of environmental change in Lake Victoria. *Palaeogeogr. Palaeoclimatol. Palaeoecol.* **119**, 215–219.

Aich V., Liersch S., Vetter T., Huang S., Tecklenburg J., Hoffmann P., Koch H., Fournet S., Krysanova V., Müller E. N. and Hattermann F. F. (2014) Comparing impacts of climate change on streamflow in four large African river basins. *Hydrol. Earth Syst. Sci.* **18**, 1305–1321.

Amogu O., Descroix L., Yéro K. S., Le Breton E., Mamadou I., Ali A., Vischel T., Bader J., Moussa I. B., Gautier E., Boubkraoui S. and Belleudy P. (2010) Increasing river flows in the Sahel? *Water* **2**, 170–199.

Azzoug M., Carré M. and Schauer A. J. (2012) Reconstructing the duration of the West African monsoon season from growth patterns and isotopic signals of shells of *Anadara senilis* (Saloum Delta, Senegal). *Palaeogeogr. Palaeoclimatol. Palaeoecol.* **346**, 145–152.

Beadle L. C. (1974) *The Inland Waters of Tropical Africa – an Introduction to Tropical Limnology*. Longman Group, London.

Bouillon S., Yambélé A., Spencer R. G. M., Gillikin D. P., Hernes P. J., Six J., Merckx R. and Borges A. V. (2012) Organic matter sources, fluxes and greenhouse gas exchange in the Oubangui River (Congo River basin). *Biogeosciences* **9**, 2045–2062.

Bouillon S., Yambélé A., Gillikin D. P., Teodoru C., Darchambeau F., Lambert T. and Borges A. V. (2014) Contrasting biogeochemical characteristics of the Oubangui River and tributaries (Congo River basin). *Sci. Rep.* **4**, 5402.

Bucini G. and Hanan N. P. (2007) A continental-scale analysis of tree cover in African savannas. *Global Ecol. Biogeogr.* **16**, 593–605.

Bullen T. D. and Kendall C. (1998) Tracing of weathering reactions and water flowpaths: a multi-isotope approach. In *Isotope Tracers in Catchment Hydrology* (eds. C. Kendall and J. J. McDonnell). Elsevier Science, Amsterdam, pp. 611–646.

Cappelaere B., Descroix L., Lebel T., Boulain N., Ramier D., Laurent J. P., Favreau G., Boubkraoui S., Boucher M., Bouzou Moussa I., Chaffard V., Hiernaux P., Issoufou H. B. A., Le Breton E., Mamadou I., Nazoumou I., Oï M., Ottlé C. and Quantin G. (2009) The AMMA-CATCH observing system in the SW Niger-site: Strategy, implementation and site description. *J. Hydrol.* **375**, 34–51.

Carroll M., Romanek C. S. and Paddock L. (2006) The relationship between the hydrogen and oxygen isotopes of freshwater bivalve shells and their home streams. *Chem. Geol.* **234**, 211–222.

Chauvaud L., Lorrain A., Dunbar R. B., Paulet Y. M., Thouzeau G., Jean F., Guarini J. M. and Mucciarone D. (2005) Shell of

the Great Scallop *Pecten maximus* as a high-frequency archive of paleoenvironmental changes. *Geochem. Geophys. Geosyst.* **6**, Q08001.

Coplen T. B. and Wassenaar L. I. (2015) LIMS for Lasers 2015 for achieving long-term accuracy and precision of δ^2H, $\delta^{17}O$, and $\delta^{18}O$ of waters using laser absorption spectrometry. *Rapid Commun. Mass Sp.* **29**, 2122–2130.

Coynel A., Seyler P., Etcheber H., Meybeck M. and Orange D. (2005) Spatial and seasonal dynamics of total suspended sediment and organic carbon species in the Congo River. *Global Biogeochem. Cy.* **19**, GB4019.

Dansgaard W. (1964) Stable isotopes in precipitation. *Tellus* **16**, 436–468.

Descroix L., Mahé G., Lebel T., Favreau G., Galle S., Gautier E., Olivry J.-C., Albergel J., Amogu O., Cappelaere B., Dessouassi R., Diedhiou A., Le Breton E., Mamadou I. and Sighomnou D. (2009) Spatio-temporal variability of hydrological regimes around the boundaries between Sahelian and Sudanian areas of West Africa: a synthesis. *J. Hydrol.* **375**, 90–102.

Descroix L., Genthon P., Amogu O., Rajot J. L., Sighomnou D. and Vauclin M. (2012) Change in Sahelian Rivers hydrograph: the case of recent red floods of the Niger River in the Niamey region. *Global Planet. Change* **98**, 18–30.

Descroix L., Ingatan A., Sighomnou D., Gautier E., Mahé G., Karambir H., Moussa I. B., Mamadou I., Noma I., Albergel J. and Olivry J. C. (2013). In *Impact of Drought and Land-Use Changes on Surface-Water Quality and Quantity: The Sahelian Paradox*. INTECH Open Access Publisher, pp. 243–271.

Dettman D. L. and Lohmann K. C. (2000) Oxygen isotope evidence for high altitude snow in the Laramide Rocky Mountains of North America during the late Cretaceous and Paleogene. *Geology* **28**, 243–246.

Dettman D. L., Reische A. K. and Lohmann K. C. (1999) Controls on the stable isotope composition of seasonal growth bands in aragonitic fresh-water bivalves (Unionidae). *Geochim. Cosmochim. Acta* **63**, 1049–1057.

Dettman D. L., Kohn M. J., Quade J., Ryerson F. J., Ojha T. P. and Hamidullah S. (2001) Seasonal stable isotope evidence for a strong Asian Monsoon throughout the last 10.7 Ma. *Geology* **29**, 31–34.

Dettman D. L., Flessa K. W., Roopnarine P. D., Schöne B. R. and Goodwin D. H. (2004) The use of oxygen isotope variation in shells of estuarine mollusks as a quantitative record of seasonal and annual Colorado River discharge. *Geochim. Cosmochim. Acta* **68**, 1253–1263.

De Wit M. and Stankiewicz J. (2006) Changes in surface water supply across Africa with predicted climate change. *Science* **311**, 1917–1921.

d'Herbè J. M. and Valentin C. (1997) Land surface conditions of the Niamey region: ecological and hydrological implications. *J. Hydrol.* **188**, 18–42.

Elliot M., Demenocal P. B., Linsley B. K. and Howe S. S. (2003) Environmental controls on the stable isotopic composition of *Mercenaria mercenaria*: potential application to paleoenvironmental studies. *Geochem. Geophys. Geosyst.* **4**(7).

Fan M. and Dettman D. L. (2009) Late Paleocene high Laramide ranges in northeast Wyoming: oxygen isotope study of ancient river water. *Earth Plan. Sci. Lett.* **286**, 110–121.

Gillikin D. P. and Bouillon S. (2007) Determination of $\delta^{18}O$ of water and $\delta^{13}C$ of dissolved inorganic carbon using a simple modification of an elemental analyzer-isotope ratio mass spectrometer (EA-IRMS): an evaluation. *Rapid Comm. Mass Spectrom.* **21**, 1475–1478.

Gillikin D. P., De Ridder F., Ulens H., Elskens M., Keppens E., Baeyens W. and Dehairs F. (2005a) Assessing the reproducibility and reliability of estuarine bivalve shells (*Saxidomus*

giganteus) for sea surface temperature reconstruction: implications for paleoclimate studies. *Palaeogeogr. Palaeoclimatol. Palaeoecol.* **228**, 70–85.

Gillikin D. P., Lorrain A., Navez J., Taylor J. W., André L., Keppens E., Baeyens W. and Dehairs F. (2005b) Strong biological controls on Sr/Ca ratios in aragonitic marine bivalve shells. *Geochem. Geophys. Geosyst.* **6**(5).

Gillikin D. P., Dehairs F., Lorrain A., Steenmans D., Baeyens W. and André L. (2006) Barium uptake into the shells of the common mussel (*Mytilus edulis*) and the potential for estuarine paleo-chemistry reconstruction. *Geochim. Cosmochim. Acta* **70**, 395–407.

Gillikin D. P., Lorrain A., Meng L. and Dehairs F. (2007) A large metabolic carbon contribution to the $\delta^{13}C$ record in marine aragonitic bivalve shells. *Geochim. Cosmochim. Acta* **71**, 2936–2946.

Gillikin D. P., Lorrain A., Paulet Y. M., André L. and Dehairs F. (2008) Synchronous barium peaks in high-resolution profiles of calcite and aragonite marine bivalve shells. *Geo-Mar. Lett.* **28**, 351–358.

Gillikin D. P., Hutchinson K. A. and Kumai Y. (2009) Ontogenic increase of metabolic carbon in freshwater mussel shells (*Pyganodon cataracta*). *J. Geophys. Res-Biogeo.* **114**(G1).

Goewert A., Surge D., Carpenter S. J. and Downing J. (2007) Oxygen and carbon isotope ratios of *Lampsilis cardium* (Unionidae) from two streams in agricultural watersheds of Iowa, USA. *Palaeogeogr. Palaeoclimatol. Palaeoecol.* **252**, 637–648.

Gonfiantini, R., Stichler, W., Rozanski, K., 1995. Standards and Intercomparison Materials Distributed by the International Atomic Energy Agency for stable isotope measurements. IAEA-Techdoc-825, pp. 13–29.

Goodwin D. H., Flessa K. W., Schöne B. R. and Dettman D. L. (2001) Cross-calibration of daily growth increments, stable isotope variation, and temperature in the Gulf of California bivalve mollusk *Chione cortezi*: implications for paleoenvironmental analysis. *Palaios* **16**, 387–398.

Goodwin D. H., Schöne B. R. and Dettman D. L. (2003) Resolution and fidelity of oxygen isotopes as paleotemperature proxies in bivalve mollusk shells: models and observations. *Palaios* **18**, 110–125.

Goodwin D. H., Cohen A. N. and Roopnarine P. D. (2010) Forensics on the half shell: a sclerochronologic investigation of a modern biological invasion in San Francisco Bay, United States. *Palaios* **25**, 742–753.

Goodwin D. H., Gillikin D. P. and Roopnarine P. D. (2013) Preliminary evaluation of potential stable isotope and trace element productivity proxies in the oyster *Crassostrea gigas*. *Palaeogeogr. Palaeoclimatol. Palaeoecol.* **373**, 88–97.

Gordillo S., Martinelli J., Cárdenas J. and Bayer M. S. (2011) Testing ecological and environmental changes during the last 6000 years: a multiproxy approach based on the bivalve *Tawera gayi* from southern South America. *J. Mar. Biol. Assoc. UK* **91**, 1413–1427.

Gröcke D. R. and Gillikin D. P. (2008) Advances in mollusc sclerochronology and sclerochemistry: tools for understanding climate and environment. *Geo-Mar. Lett.* **28**, 265–268.

Grossman E. L. and Ku T. L. (1986) Oxygen and carbon isotope fractionation in biogenic aragonite-temperature effects. *Chem. Geol.* **59**, 59–74.

Haag W. R. and Commens-Carson A. M. (2008) Testing the assumption of annual shell ring deposition in freshwater mussels. *Can. J. Fish. Aquat. Sci.* **65**, 493–508.

Hijmans R. J., Cameron S. E., Parra J. L., Jones P. G. and Jarvis A. (2005) Very high resolution interpolated climate surfaces for global land areas. *Int. J. Climatol.* **25**, 1965–1978.

Hulme M., Doherty R., Ngara T., New M. and Lister D. (2001) African climate change: 1900–2100. *Clim. Res.* **17**, 145–168.

Itiveh K. O. and Bigg G. R. (2008) The variation of discharge entering the Niger Delta system, 1951–2000, and estimates of change under global warming. *Int. J. Climatol.* **28**, 659–666.

Ivany L. C., Wilkinson B. H. and Jones D. S. (2003) Using stable isotopic data to resolve rate and duration of growth throughout ontogeny: an example from the surf clam. *Spisula solidissima. Palaios* **18**, 126–137.

Kaandorp R. J. G., Vonhof H. B., Del Busto C., Wesselingh F. P., Ganssen G. M., Marmo'l A. E., Romero Pittman L. and van Hinte J. E. (2003) Seasonal stable isotope variation of the Amazonian freshwater bivalve *Anodontites trapesialis. Palaeogeogr. Palaeoclimatol. Palaeoecol.* **194**, 339–354.

Kaandorp R. J. G., Wesselingh F. P. and Vonhof H. B. (2006) Ecological implications from stable isotope records of Miocene western Amazonian bivalves. *J. S. Am. Earth Sci.* **21**, 54–74.

Kesler D. H. and Bailey R. C. (1993) Density and ecomorphology of a freshwater mussel (*Elliptio complanata*, Bivalvia: Unionidae) in a Rhode Island Lake. *J. N. Am. Benthol. Soc.* **12**, 259–264.

Kesler D. H., Newton T. J. and Green L. (2007) Long-term monitoring of growth in the Eastern Elliptio, *Elliptio complanata* (Bivalvia: Unionidae), in Rhode Island: a transplant experiment. *J. N. Am. Benthol. Soc.* **26**, 123–133.

Klein R. T., Lohmann K. C. and Thayer C. W. (1996) Bivalve skeletons record sea-surface temperature and δ^{18}O via Mg/Ca and ^{18}O/^{16}O ratios. *Geology* **24**, 415–418.

Kryger J. and Riisgård H. U. (1988) Filtration rate capacities in 6 species of European freshwater bivalves. *Oecologia* **77**, 34–38.

Laraque A., Mahé G., Orange D. and Marieu B. (2001) Spatiotemporal variations in hydrological regime within Central Africa during the XXth century. *J. Hydrol.* **245**, 104–117.

Lawrence D. and Vandecar K. (2015) Effects of tropical deforestation on climate and agriculture. *Nature Clim. Change* **5**, 27–36.

Leblanc M. J., Favreau G., Massuel S., Tweed S. O., Loireau M. and Cappelaere B. (2008) Land clearance and hydrological change in the Sahel: SW Niger. *Global Planet. Change* **61**, 135–150.

Leduc C., Favreau G. and Schroeter P. (2001) Long term rise in a Sahelian water-table: the Continental Terminal in South-West Niger. *J. Hydrol.* **243**, 43–54.

Lorrain A., Paulet Y. M., Chauvaud L., Dunbar R., Mucciarone D. and Fontugne M. (2004) δ^{13}C variation in scallop shells: Increasing metabolic carbon contribution with body size? *Geochim. Cosmochim. Acta* **68**, 3509–3519.

Mahé G. and Paturel J. E. (2009) 1896–2006 Sahelian annual rainfall variability and runoff increase of Sahelian rivers. *C.R. Geosciences* **341**, 538–546.

Mahé G., Lienou G., Descroix L., Bamba F., Paturel J. E., Laraque A., Meddi M., Habaieb H., Adeaga O., Dieulin C., Chahnez Kotti F. and Khomsi K. (2013) The rivers of Africa: witness of climate change and human impact on the environment. *Hydrol. Process.* **27**, 2105–2114.

Mayaux P., Richards T. and Janodet E. (1999) A vegetation map of Central Africa derived from satellite imagery. *J. Biogeogr.* **26**, 353–366.

McConnaughey T. A. and Gillikin D. P. (2008) Carbon isotopes in mollusk shell carbonates. *Geo Mar. Lett.* **28**, 287–299.

McConnaughey T. A., Burdett J., Whelan J. F. and Paull C. K. (1997) Carbon isotopes in biological carbonates: respiration and photosynthesis. *Geochim. Cosmochim. Acta* **61**, 611–622.

Mook W. and Rozanski K. (2000) Environmental isotopes in the hydrological cycle. *IAEA and UNESCO, Technical Documents Hydrol.* **39**.

Mook W. G. and Tan F. C. (1991) Stable carbon isotopes in rivers and estuaries. In *Biogeochemistry of Major World Rivers* (eds. E. T. Degens, S. Kempe and J. E. Richey). Wiley, Chichester, pp. 245–264.

Mueller-Lupp T., Erlenkeuser H. and Bauch H. A. (2003) Seasonal and interannual variability of Siberian river discharge in the Laptev Sea inferred from stable isotopes in modern bivalves. *Boreas* **32**, 292–303.

Negrel P. and Dupre B. (1993) *Temporal Variations of Sr Isotopic Ratios, Major and Trace Elements Composition of the Oubangui River Basin: Implications for the Source of Material*. Grands Bassins Fluviaux, Paris, 22-24 November 1993.

Nguimalet C. R. and Orange D. (2013) Dynamique hydrologique récente de l'Oubangui à Bangui (Centrafrique): impacts anthropiques ou climatiques? *Geo-Eco-Trop* **37**, 101–112.

Nicholson S. E. (2000) The nature of rainfall variability over Africa on time scales of decades to millenia. *Glob. Planet. Change* **26**, 137–158.

O'Neil D. D. and Gillikin D. P. (2014) Do freshwater mussel shells record road-salt pollution? *Sci. Rep.* **4**, 7168.

O'Donnell T. H., Macko S. A., Chou J., Davis-Hartten K. L. and Wehmiller J. F. (2003) Analysis of δ^{13}C, δ^{15}N, and δ^{34}S in organic matter from the biominerals of modern and fossil *Mercenaria* spp.. *Org. Geochem.* **34**, 165–183.

Olomoda I. A. (2012) Challenges of Continued river Niger low flow into Nigeria. *Special Publ. Nigerian Assoc. Hydrol. Sci.*, 145–155.

Orange D., Wesselink A. J., Mahé G. and Feizoure C. T. (1997) The effects of climate changes on river baseflow and aquifer storage in Central Africa. *Sustain. of Water Resources under Increas. Uncertainty IAHS Publ.* **240**, 113–123.

Probst J. L., Mortatti J. and Tardy Y. (1994) Carbon river fluxes and weathering CO_2 consumption in the Congo and Amazon river basins. *Appl. Geochem.* **9**, 1–13.

Ricken W., Steuber T., Freitag H., Hirschfeld M. and Niedenzu B. (2003) Recent and historical discharge of a large European river system–oxygen isotopic composition of river water and skeletal aragonite of *Unionidae* in the Rhine. *Palaeogeogr. Palaeoclimatol. Palaeoecol.* **193**, 73–86.

Romanek C. S., Grossman E. L. and Morse J. W. (1992) Carbon isotopic fractionation in synthetic aragonite and calcite: effects of temperature and precipitation rate. *Geochim. Cosmochim. Acta* **56**, 419–430.

Runge J. and Nguimalet C. R. (2005) Physiogeographic features of the Oubangui catchment and environmental trends reflected in discharge and floods at Bangui 1911–1999, Central African Republic. *Geomorphology* **70**, 311–324.

Sankaran M., Hanan N. P., Scholes R. J., Ratnam J., Augustine D. J., Cade B. S., Gignoux J., Higgins S. I., Le Roux X., Ludwig F. and Ardo J. (2005) Determinants of woody cover in African savannas. *Nature* **438**, 846–849.

Snoussi M., Kitheka J., Shaghude Y., Kane A., Arthurton R., Le Tissier M. and Virji H. (2007) Downstream and coastal impacts of damming and water abstraction in Africa. *Environ. Manage.* **39**, 587–600.

Stroppiana D., Boschetti M., Brivio P. A., Nutini F. and Bartholomé E. (2011) Analysis of earth observation time series to investigate the relation between rainfall, vegetation dynamic and streamflow in the Uele basin (Central African Republic). In *Analysis of Multi-temporal Remote Sensing Images (MultiTemp), 2011 6th International Workshop on the*. IEEE, pp. 177–180.

Versteegh E. A., Troelstra S. R., Vonhof H. B. and Kroon D. (2009) Oxygen isotope composition of bivalve seasonal growth increments and ambient water in the rivers Rhine and Meuse. *Palaios* **24**, 497–504.

Versteegh E. A., Vonhof H. B., Troelstra S. R., Kaandorp R. J. and Kroon D. (2010) Seasonally resolved growth of freshwater bivalves determined by oxygen and carbon isotope shell chemistry. *Geochem. Geophys. Geosyst.* **11**, Q08022.

Versteegh E. A., Vonhof H. B., Troelstra S. R. and Kroon D. (2011) Can shells of freshwater mussels (Unionidae) be used to estimate low summer discharge of rivers and associated droughts? *Int. J. Earth Sci.* **100**, 1423–1432.

Vonhof H. B., Joordens J. C., Noback M. L., van der Lubbe J. H., Feibel C. S. and Kroon D. (2013) Environmental and climatic control on seasonal stable isotope variation of freshwater molluscan bivalves in the Turkana Basin (Kenya). *Palaeogeogr. Palaeoclimatol. Palaeoecol.* **383**, 16–26.

Wanamaker A. D., Kreutz K. J., Borns H. W., Introne D. S., Feindel S., Funder S., Rawson P. D. and Barber B. J. (2007) Experimental determination of salinity, temperature, growth, and metabolic effects on shell isotope chemistry of *Mytilus edulis* collected from Maine and Greenland. *Paleoceanography* **22**.

Wassenaar L. I., Coplen T. B. and Aggarwal P. K. (2014) Approaches for achieving long-term accuracy and precision of $\delta^{18}O$ and δ^2H for waters analyzed using laser absorption spectrometers. *Environ. Sci. Technol.* **48**, 1123–1131.

Wesselink A. J. and Orange D. (1996) Les régimes hydroclimatiques et hydrologiques d'un bassin versant de type tropical humide: l'Oubangui (République Centrafricaine), *L'hydrologie tropicale: géoscience et outil pour le développement (Actes de la conférerice de Paris, mai 1995)*. *IAHS Publ.* **238**, 179–194.

Yan L., Schöne B. R. and Arkhipkin A. (2012) *Eurhomalea exalbida* (Bivalvia): a reliable recorder of climate in southern South America? *Palaeogeogr. Palaeoclimatol. Palaeoecol.* **350**, 91–100.

Zanchetta G., Leone G., Fallick A. E. and Bonadonna F. P. (2005) Oxygen isotope composition of living land snail shells: data from Italy. *Palaeogeogr. Palaeoclimatol. Palaeoecol.* **223**, 20–33.

Associate editor: Claire Rollion-Bard